

UNIVERSITA' DEGLI STUDI DI MILANO-BICOCCA
FACOLTA' DI MEDICINA E CHIRURGIA

DOTTORATO DI RICERCA IN EMATOLOGIA SPERIMENTALE
(XXV ciclo)

Coordinatore: Prof. Carlo Gambacorti Passerini

TESI DI DOTTORATO DI RICERCA

**Mass spectrometry-based serum Protein Profiling
at population level: serum hepcidin and beyond**

Relatore:

Prof. Domenico Girelli

Università degli Studi di Verona

Dottorando in Ricerca:

Dott.ssa Michela Corbella

ANNO ACCADEMICO 2012-2013

TABLE OF CONTENTS

1. ABSTRACT

2. ABBREVIATIONS

3. INTRODUCTION

3.1 Iron metabolism and Heparidin

3.2 Heparidin assays

3.3 The Val Borbera Project - Iron section

3.4 Protein Profiling analysis

3.5 Further proteomics analyses of the SPI

4. AIM OF THE THESIS

5. MATERIALS AND METHODS

5.1 Val Borbera Project

5.1.1 Study subjects

5.1.2 Blood tests

5.1.3 Serum hepcidin assay

5.1.4 Statistical analysis

5.2 Protein Profiling analysis

5.2.1 Subjects

5.2.2 Analysis

5.2.3 Lucid Proteomics System

5.3 Co-Immunoprecipitation (Co-IP) experiments

5.3.1 Serum samples selection

5.3.2 Co-IP protocol

5.3.3 Immunoblotting analysis

6. RESULTS AND DISCUSSION

6.1 Val Borbera Project

6.1.1 Heparidin-25 analysis in VB population

6.1.2 Heparidin-20 analysis in VB population

6.2 Profiling analysis

6.2.1 SPI fragments – Identification and speculations

6.2.2 Bioinformatics analysis

6.3 Co-IP experiments

7. CONCLUSIONS

REFERENCES

1. ABSTRACT

Iron is essential for multiple biological functions and its plasma levels have to be tightly regulated. Hepcidin, a peptide hormone produced by liver, is the main regulator of iron homeostasis and its altered production is related to functional iron deficiency (high hepcidin levels) or iron overload (hepcidin deficiency). The first part of the project here described is the quantification of serum hepcidin levels in the Val Borbera (VB) population, a genetic isolate living in Northern Italy, as part of a larger project started in 2005 for a demographic and epidemiological analysis. Serum hepcidin measurements were performed in our lab by a validated mass spectrometry-based method i.e. Surface-Enhanced Laser Desorption/Ionization Time-of-Flight Mass Spectrometry (SELDI-TOF-MS). This technique allowed also the discrimination and quantification of a truncated hepcidin isoform, hepcidin-20, that has been studied for the first time at population level. In the second part of the project it is described the use of the SELDI platform for proteome profiling analysis, comparing spectra of subjects affected by iron disorders with those of healthy controls. Differentially expressed peptides, representing putative novel biomarkers have been further studied, as described in the third part of the work, both by classic proteomics (co-immunoprecipitation and Western blotting) and bioinformatics approaches, in order to confirm results and gain insight about the molecular pathway involved. The results of the projects here presented, like the establishment of a reference range for hepcidin-25 levels and the discovery of a putative novel biomarker of iron homeostasis diseases, could have clinical applications, both at diagnostic and therapeutic levels.

2. ABBREVIATIONS

BMP	Bone morphogenetic protein
CKD	Chronic kidney disease
Co-IP	Co-immunoprecipitation
CRP	C-reactive protein
FPN	Ferroportin
GDF-15	Growth differentiation factor-15
HAMP	Hepcidin
HH	Hereditary haemochromatosis
HJV	Hemojuvelin
IDA	Iron deficiency anaemia
IL-6	Interleukin-6
IO	Iron overload
IRIDA	Iron Refractory Iron Deficiency Anaemia
JAK	Janus kinase
MDS	Myelodysplastic syndromes
MT-2	Matriptase-2
ROC	Receiver operator characteristic
SELDI-TOF-MS	Surface Enhanced Laser desorption Ionization-Time of Flight-Mass Spectrometry
SMAD	Son of mothers against decapentaplegic
SPI	Serin protease inhibitor
STAT3	Signal transducer and activator of transcription 3
TfR1	Transferrin receptor 1
TfR2	Transferrin receptor 2
Tf-Fe ₂	Diferric transferrin
TMPRSS6	Transmembrane protease serine 6
VB	Val Borbera
VIT	Vault protein inter-alpha-trypsin
vWA	von Willebrand factor type A

3. INTRODUCTION

3.1 Iron Metabolism and Hepcidin

Iron is essential for multiple biological functions. It is a component of cytochromes, many enzymes and more than two thirds of the body's iron content is incorporated in haemoglobin (Andrews, 1999). Disorders of iron metabolism are among the most common diseases of humans (Hentze et al., 2010). Both iron deficiency and iron overload can be deleterious. In the latter case, in fact, iron excess can cause oxidative stress and cell damage. Therefore, plasma iron levels are maintained within narrow limits and are tightly regulated, being modulated by signals from iron consuming pathways, such as erythropoiesis, and sending signals to cells supplying iron to the blood stream. Iron is released into the circulation by enterocytes, that absorb dietary iron, and by macrophages, that recycle iron from senescent erythrocytes (Hentze et al., 2010).

Hepatocytes have a role in iron metabolism as major site of iron storage and synthesis of hepcidin, a peptide identified as the systemic iron-regulatory hormone. Hepcidin regulates iron efflux into the circulation by inhibiting its release from enterocytes, macrophages and hepatocytes, through the binding to and subsequent internalization of its receptor ferroportin, the only known cellular iron exporter (Nemeth et al., 2004). Multiple stimuli converge on the regulation of hepcidin production, like erythropoiesis, body iron stores and inflammatory/host defense (Ganz and Nemeth, 2012) (Figure 1).

Hepcidin expression is regulated at transcriptional level (Flanagan et al., 2007) by multiple signals including systemic iron availability (in the form of diferric transferrin, Tf-Fe₂), hepatic iron stores, erythropoietic activity, hypoxia and inflammatory/infectious states (Hentze et al., 2010).

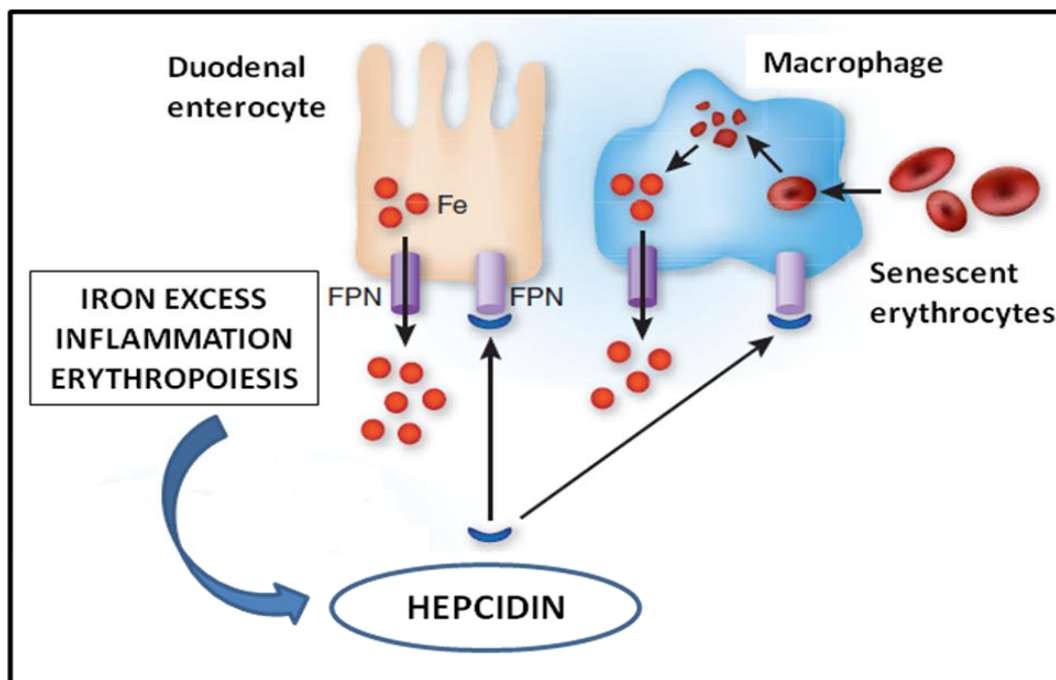


Figure 1. Regulation of hepcidin synthesis and action. Hepcidin is synthesized in the liver, responding to increased iron levels in the serum, inflammatory and also to erythropoietic demand. Hepcidin acts inhibiting iron absorption from the duodenum and iron recycling from macrophages, leading ferroportin degradation. (adapted from Camaschella, 2009)

Hepcidin regulation by extracellular iron involves transferrin receptor 1 and 2 (TfR1 and TfR2), acting as sensors of Tf-Fe₂ concentration on the plasma membrane of hepatocytes, and HFE, another membrane protein acting as an intermediary between the two molecules. According to current model, high concentrations of Tf-Fe₂ displace HFE from TfR1, to promote its interaction with TfR2, and so the HFE-TfR2 complex activates hepcidin transcription (Figure 2). Also the bone morphogenetic protein (BMP) pathway is involved in hepcidin regulation by iron; in particular BMP6, upregulated by hepatic iron stores, is the activating ligand of the BMP receptor, and controls hepcidin expression through the SMAD (Son of Mothers Against Decapentaplegic) pathway (Ganz, 2011) (Figure 2). Hemojuvelin (HJV), a membrane anchored co-receptor for BMP receptor (Babitt et al., 2006), is another component essential for iron homeostasis, since its mutations result in severe hepcidin deficiency and have been shown to be the main cause

of juvenile hemochromatosis (Papanikolaou et al., 2004). HJV is iron specific and increases the sensitivity of BMP receptor to BMPs (Ganz, 2011). Another membrane protein, matriptase-2 (MT2, also called transmembrane protease serine 6 or TMPRSS6), negatively regulates hepcidin expression by cleavage of HJV (Silvestri et al., 2008).

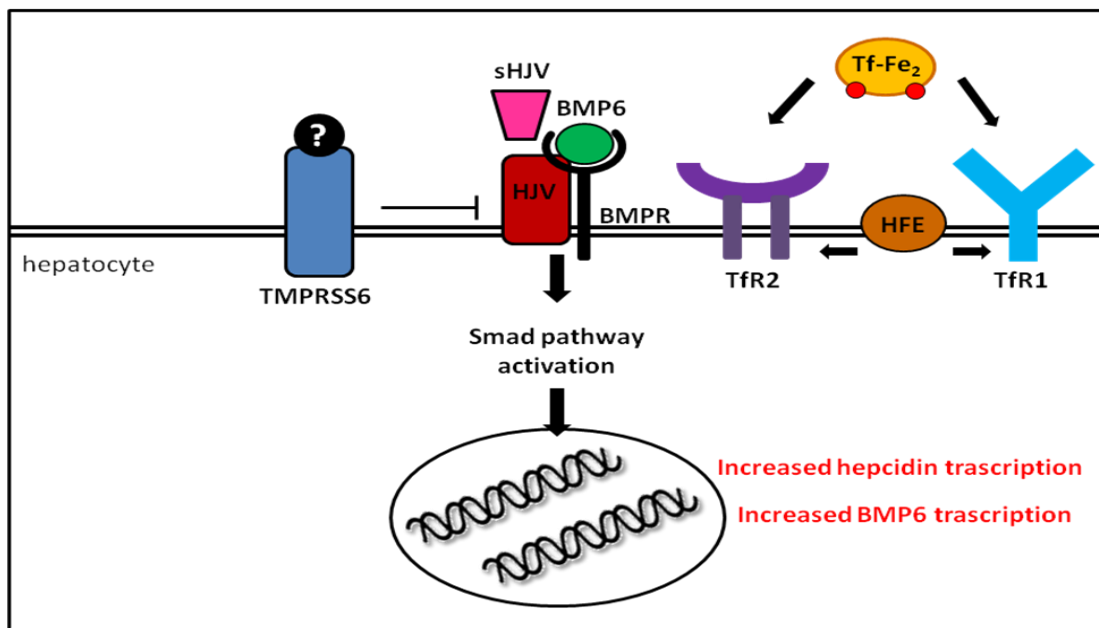


Figure 2. Hepcidin regulation by iron. Iron is represented by holotransferrin (Tf-Fe₂). High Tf-Fe₂ levels displace HFE from TfR1, promoting its interaction with TfR2. TfR2 and HFE increase the sensitivity of the BMP receptor to its ligands, perhaps by its interactions with HJV. HJV, interacting with BMPR, activates SMAD pathway and induces an increased hepcidin and BMP6 expression. (adapted from Hentze et al., 2010)

Mutations in genes encoding proteins involved in hepcidin regulation result either in hepcidin deficiency, with consequent iron overload, or in hepcidin excess, causing iron deficiency (Ganz, 2011). Mutations of *HFE*, *TfR2*, *HJV* and of hepcidin gene itself (*HAMP*) causes hereditary haemochromatosis (HH), a disease characterized by inappropriately high iron absorption and low/undetectable hepcidin levels. More rarely mutations affect *Fpn*, the downstream hepcidin receptor; those cases are characterized by iron load and high levels of hepcidin. Mutations of *Tmprss6*, encoding the liver expressed hepcidin inhibitor

serine protease matriptase-2, cause iron refractory iron deficiency anaemia (IRIDA), with severe iron deficiency and inappropriate high hepcidin levels (Ganz, 2011).

Hepcidin is regulated also by erythropoiesis, which has a negative effect on its expression, in order to increase circulating iron levels. This effect is evident in β -thalassemia, where an ineffective erythropoiesis leads to a massive expansion of erythrocytes precursors, determining low hepcidin levels (Adamsky et al., 2004, Papanikolaou et al., 2005). Growth differentiation factor-15 (GDF-15) is detectable at high levels in serum of β -thalassemic patients (Tanno et al., 2007) and in cell models showed suppression of hepcidin transcription. However, the precise underlying molecular mechanism has not yet been characterized (Hentze et al., 2010). Indeed, the same authors (Tanno et al., 2010) demonstrated later that low GDF-15 levels are present in blood donors affected by iron deficiency, indicating the presence of an erythroid suppressor of hepcidin different from GDF-15.

Hepcidin transcription is induced during inflammation and infections by increased levels of cytokines like interleukin-6 (IL-6) and interleukin-1 (IL-1). It has been shown that the interaction of IL-6 with its receptor activates the janus kinase (JAK)/signal transducer and activator of transcription-3 (STAT3) signaling pathway (Nemeth et al., 2004, Pietrangelo et al., 2007, Verga Falzacappa et al., 2007, Wrighting and Andrews, 2006). An early hypoferrremia is associated to inflammation-induced hepcidin increase, which could be explained as a mechanism of host defense. Indeed, iron is sequestered in order to limit its availability to iron-dependent pathogens, although it is less available for erythropoietic demand as well, leading to the so called anaemia of inflammation (Ganz and Nemeth, 2012).

3.2 Hepcidin Assays

The development of a reliable assay for hepcidin quantification is of great interest in order to improve our understanding of iron homeostasis disorders, with important implications regarding diagnosis and clinical management of such diseases (Kroot et al., 2011). Hepcidin quantification is difficult due to its tendency to aggregate (Hunter et al., 2002) and stick to laboratory plastics. Moreover difficulties have been encountered in the development of specific antihepcidin antibodies for immunological assays, due to its small and compact structure, and to its high degree of conservation among different species. Moreover the presence of truncated hepcidin isoforms like hepcidin-22 and hepcidin-20 impairs the antibody specificity for the bioactive form, i.e. hepcidin-25. The first-generation hepcidin assays were an immunodot assay (Nemeth et al., 2004), and a SELDI-TOF mass spectrometry assay (Kemna et al., 2005, Kemna et al., 2007, Tomosugi et al., 2006), but they were both just semiquantitative. Recent advances have been made by introducing an internal standard for an absolute quantification of hepcidin-25 in serum and urine by a second generation mass spectrometry assay (Kroot et al., 2010, Swinkels et al., 2008). Advances have been made also in exploring some ELISA assays (Kroot et al., 2010). Immunological assays could be easily used in clinical laboratories while MS assays require skilled dedicated personnel and relatively expensive equipment. Despite this, the first ones will measure the total hepcidin concentrations (i.e. likely including both major and minor isoforms), while the latter ones are able to distinguish between the bioactive form and the truncated isoforms. Our lab has contributed significantly to the set up and improvement of hepcidin MS assay (Castagna et al., 2010).

3.3 The Val Borbera Project - Iron section

Our lab took part in one of the first large scale epidemiological and genetic study of serum hepcidin in an adult population; the latter was recruited in the Val Borbera, a genetic isolate in Northern Italy (Figure 3), that has been previously well described (Traglia et al., 2009).



Figure 3. Borbera Valley geographical location.

The iron section of this project aimed to the definition of a solid reference range for serum hepcidin levels, as a function of age, gender and physiological status with important diagnostic insights about disorders of iron metabolism. A second aim was the definition of the heritability of serum hepcidin, that is the estimation of the relative influence of genetic and non-genetic factors on hepcidin variation at population level. Moreover, we aimed at the definition of possible predictors of serum hepcidin levels among the wide panel of parameters recorded in the database of the Val Borbera Project. A Genome-wide association study was also planned by our collaborators involved in this study, in order to discover new genes taking part in hepcidin modulation, and/or confirm previously known candidate genes. This analysis could contribute to improve our

knowledge regarding the pathophysiology of disorders of iron metabolism, and is currently under definition.

Serum hepcidin measurements were performed by a validated mass spectrometry-based method, i.e. SELDI-TOF-MS (Swinkels et al., 2008) with recent technical improvements, suitable for high-throughput analysis and for relatively fast analysis of the large number of samples (at least 1725 subjects) from the Val Borbera biobank. As noted above, hepcidin-25, the bioactive form, undergoes proteolytic cleavage generating two truncated isoforms, hepcidin-22 (hep-22) and hepcidin-20 (hep-20), existing in biological fluids whose physiological role is still unclear (Park et al., 2001; Castagna et al., 2010). Mass spectrometry, unlike immunological assays, has the advantage to discriminate between the different isoforms, and allows to detect low levels of hep-20 in both serum and urine, while hep-22 has been found only in urine (Kemna et al., 2007). Functional studies have demonstrated that the two truncated hepcidin isoforms are not able to interact with ferroportin (Nemeth et al., 2006), indicating that they're not actively involved in iron regulation. They have been generally considered as degradation byproducts of hep-25. However, recent studies showed that hep-20 has greater antimicrobial and fungicidal activity than hep-25, particularly at acidic pH (Maisetia et al., 2010, Tavanti et al., 2011). Relatively high levels of hep-20 have been found in heterogeneous pathological conditions like acute myocardial infarction (AMI) (Suzuki et al., 2009), anemia of chronic disease (ACD) (Tomosugi et al., 2006) and, particularly, in chronic kidney disease (CKD) (Campostrini et al., 2010, Peters et al., 2010, Tessitore et al., 2010). For example, in our lab we also measured hep-20 by SELDI-MS in 54 patients in chronic hemodialysis, and it was detected in 100%, compared to 39% of the

corresponding controls (Campostrini et al., 2010). Also Kroot et al (Kroot et al., 2010) found by a weak cation exchange (WCX)-TOF-MS assay, relevant amount of hep-20 in some patients, again particularly in CKD. So the contribution of hep-20 to total serum hepcidin is not constant and may vary substantially between healthy subjects and patients with different diseases. We present here our work that took advantage of the VB study for the first quantification in a large population of serum hep-20 concentration, described in relation to age and sex, together with its determinant, and the variation of hep-25:hep-20 ratio according to the iron status (Traglia et al., 2011, Campostrini et al., 2012).

3.4 Protein Profiling analysis

Protein biomarker discovery is a growing branch of proteomics having as a major tool differential expression analysis or profiling, which compares protein expression levels across samples in order to reveal expression patterns correlated with particular biological states. Differentially expressed proteins can be used as biomarkers to classify organisms, disease states, metabolic conditions or responses to environmental or chemical challenges. Biomarkers discovery has several potential applications such as understanding disease pathology and thereby developing drugs, disease diagnosis, prognosis and helping for the choice of effective treatment. Obstacles to biomarker discovery are the sample complexity, for example in serum/plasma, and small changes in protein levels. Moreover in samples like serum, another problem is the accessibility to low abundant proteins and small peptides, particularly in presence of high-abundance proteins (Walsh et al., 2010). The approaches based on mass spectrometry can be

classified into two main categories: bottom-up and top-down approaches. In the first one a complex peptide mixture is produced by digestion of sample proteins using a proteolytic enzyme, followed by the analysis by liquid chromatography and tandem mass spectrometry (LC-MS/MS). In top-down methods intact proteins are analyzed, and consists of a first separation step, using liquid or surface chromatography or 2-D gel electrophoresis, which reduces the biological complexity, followed by differential expression analysis. Thus spots, fractions or peaks predicted as candidate biomarkers are identified by mass spectrometry.

In our analysis the ProteinChip SELDI platform has been used, exploiting chromatographic arrays (ProteinChip arrays) with chemically treated surfaces for separation of proteins based on physiochemical properties. Unbound proteins and other substances are washed away, reducing the biological complexity. Differential expression analysis is then performed by mass spectrometry, which in our analysis has been performed by the ProteinChip SELDI reader, reporting mass and average quantity of proteins present in the sample. This technique allows sensitive measurements of relatively small changes in protein expression levels and can process large numbers of samples, needed to increase the statistical significance of a potential biomarker. The ProteinChip SELDI Software has been used to manage and analyze the data. It includes algorithms that group peaks across all the spectra and display statistical differences in protein/peptide expression level. It also provides univariate statistics in the form of p-values and receiver-operator characteristic (ROC) curves, to assess diagnostic value (sensitivity and specificity). SELDI profiling has been widely applied as a powerful method for cancer research (diagnosis strategies) as well as biomarker discovery (Issaq et al., 2002, Miyamae et al., 2005,

Petricoin and Liotta, 2004, Xiao et al., 2004). Once a set of manageable number of proteins showing quantitative changes between diseased samples and appropriate controls is defined, further complementary experimental approaches are needed to test their function (Cravatt et al., 2007). This approach can be very useful in the understanding of the molecular basis of cellular and physiological processes involved in the pathogenesis of studied diseases.

Potential limitations of these comparative studies could be represented by differences in storage duration and age between cases and controls. Standard procedures should be in fact used for handling and processing all the samples (van Winden et al., 2009). For the same reason it's difficult to compare results of experiments performed in different laboratories. Moreover, in order to obtain biomarkers reaching the statistical significance a large cohort of subjects is required for the analysis, and the use of multiple markers is necessary to improve the specificity and so the discrimination of disease subjects. In order to confirm the clinical value of candidate biomarkers it is required to reproduce the results of the differential analysis on larger cohort of subjects and also conduct pilot studies using immunoassay approaches to confirm the up- or down-regulation of each marker.

Not all the components of the hepcidin-regulatory apparatus have been identified (Ganz, 2011), and proteomics profiling analysis could be a suitable tool for the discovery of unknown regulators involved in iron homeostasis pathologies. To this purpose we used the SELDI platform to analyze spectra of subjects affected by different iron disorders, i.e. iron deficiency anaemia (IDA) and iron overload (IO), selected among Val Borbera pool, that we compared with healthy subjects selected from the same pool. We also analyzed

subjects affected by Myelodysplastic syndromes (MDSs) analyzed in a previous study (Santini et al., 2011) and patients with inflammatory conditions hospitalized at the Internal Medicine Unit ward in Verona. Among the peptides/proteins resulted from those analysis, some could be attributed to the fragmentation of a serin protease inhibitor (SPI), differentially expressed in all of the diseases. This protein was then studied with further complementary experiments to confirm its role in iron metabolism.

3.5 Further proteomic analyses of the SPI

The SPI is an acute phase protein which was firstly cloned and characterized in 1995, as plasma kallikrein sensitive glycoprotein, by two groups (Nishimura et al., 1995, Saguchi et al., 1995). It belongs to a family of protease inhibitors composed of a common light chain, *i.e.* bikunin (contributing to the protease inhibitory activity), and many closely related heavy chains (HCs) (Zhuo et al., 2004). They are mainly secreted by the liver and present in blood at high concentration. Conversely from all the other components, SPI does not bind bikunin and exists as a free HC isoform in blood circulation (Zhuo and Kimata, 2008). It contains a vault protein inter- α -trypsin inhibitor domain (VIT) and a von Willebrand factor type A I α I domain (vWA). Importantly, the conserved DPFHII sequence typical of the other isoforms belonging to the family, is absent in this SPI (Song et al., 2006). At present, little information is known about SPI behaviors and biological function. It is readily cleaved, by plasma kallikrein, into the N-terminal 85 kDa and the C-terminal 35 kDa fragments. The N-terminal fragment is then further cleaved to the N-terminal Mr 57 kDa fragment and a putative 28 kDa fragment (Choi-Miura et al., 1995, Pu et al., 1994) which covers 65% of the proline-rich region and has never been detected, suggesting a

rapid cleavage into smaller fragments (Song et al., 2006) (Figure 4). Some previous reports highlighted the presence of several fragments derived from this region by using a SELDI-TOF-MS approach (Fung et al., 2005, Song et al., 2006, Zhang et al., 2004).

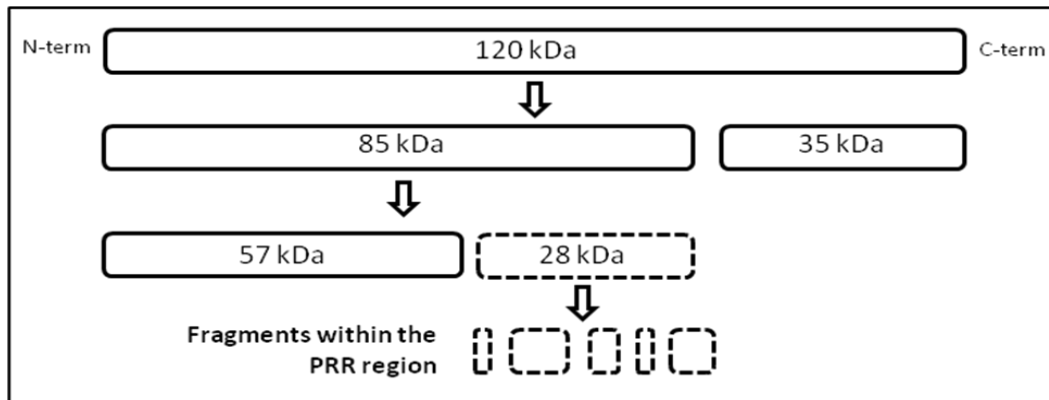


Figure 4. Model of SPI cleavage. Dashed boxes represent the uncharacterized fragments (Song et al., 2006).

Furthermore these fragments were related to the detection of early stage ovarian cancer (Zhang et al., 2004) or associated with different types of cancer (Fung et al., 2005, Song et al., 2006). Interestingly not only the fragmentation patterns were different among different diseases but also some fragments were significantly increased or decreased in patients with different types of diseases (Song et al., 2006). Some of these fragments were also shown to be related to other types of cancer such as melanoma and breast cancer (Caputo et al., 2005), pancreatic cancer (Koomen et al., 2005) or prostate, bladder and breast cancer (Villanueva et al., 2006).

4. AIM OF THE THESIS

- Definition of a solid reference range for serum hepcidin-25 levels, by its quantification in the large genetic isolate of VB population using SELDI-TOF-MS, taking into account possible predictors of serum hepcidin levels among the wide panel of parameters recorded in the referring database.
- Detection of hepcidin-20 isoform levels in the same cohort of VB population and evaluation of its possible predictors.
- Profiling analysis of selected subset of subjects affected by different disorders of iron homeostasis (such as iron overload and iron deficiency anemia) for the discovery of new potential biomarkers of such pathological conditions and/or novel components of the regulatory pathways of iron metabolism.
- Characterization and bioinformatics analysis of a putative biomarker (SPI), possibly involved in hepcidin regulation, and of its interaction with an already known hepcidin negative regulator in the frame of iron metabolism network.

5. MATERIALS AND METHODS

5.1 Val Borbera Project

5.1.1 Study subjects

The VB population has been previously described in details (Traglia et al., 2009). Only individuals aged 18 years or older were eligible to participate in the study. The study was approved by the San Raffaele Hospital and Regione Piemonte ethical committees.

5.1.2 Blood tests

Fasting blood samples were obtained early in the morning and stored at -80°C. Blood cell counts and erythrocyte indexes were determined with an automated cell counter (Sala et al., 2008). Other blood tests, serum iron, transferrin and ferritin were determined by standard methods. Transferrin saturation was calculated dividing serum iron by transferrin (mg/dl) x1.24 (Piperno, 1998).

5.1.3 Serum hepcidin assay

Serum hepcidin isoforms were measured with a mass spectrometry based method validated in our lab, that is surface enhanced laser desorption/ionization time-of-flight mass spectrometry (SELDI-TOF-MS) using a PCS4000 (Bio-Rad, Hercules, California, USA) mass spectrometer. The sample was loaded onto copper loaded immobilized metal affinity capture ProteinChip arrays (IMAC30-Cu²⁺) that binds hepcidin based on its affinity for Cu²⁺ ions. A synthetic hepcidin (hepcidin-24, Peptide International, Louisville, Kentucky, USA) was used as internal standard for absolute quantification. Hepcidin-24 is 2673.9 Da, and it is clearly distinguishable from hep-25 (2789 Da) by TOF MS. Moreover, it is suitable as internal standard since has similar chromatographic binding and flying

characteristics as the natural hepcidin isoforms. With respect to hep-20 quantification, we used as reference peak hep-20 kindly provided by Dr. Elizabeta Nemeth (University of California Los Angeles, CA). All binding surfaces were equilibrated and washed with appropriate buffers according to the manufactures instructions (Bio-Rad, Hercules, CA) and protein chip handling was performed in a nitrogen atmosphere to prevent methionine oxidation of serum hepcidin. The focus mass for ProteinChip reading with mass spectrometer was set at 2800 Da, a mass value close to hepcidin mass. To calculate the absolute serum hep-25 and hep-20 concentration the following equations were applied respectively:

$$\frac{(\text{sample 2789 m/z peak intensity}) \times 10 \text{ nM}}{(\text{hepc24 spiked sample 2673 m/z peak intensity} - \text{non spiked sample 2673 m/z peak intensity})}$$

$$\frac{(\text{sample 2192 m/z peak intensity}) \times 10 \text{ nM}}{(\text{hepc24 spiked sample 2673 m/z peak intensity} - \text{non spiked sample 2673 m/z peak intensity})}.$$

The lower limit of detection for both hep-25 and hep-20 was 0.55 nM.

5.1.4 Statistical analysis

Statistical analysis were performed by STATA V.9 (StatCorp) or by SPSS 17.0 software (SPSS Inc., Chicago, IL, USA). Comparisons of all measured parameters in men and women were performed using the t-test. Sex specific correlation analysis was used to evaluate the relationship between serum hepcidin and all other parameters. Subsequently, simple and multiple linear regression analysis were employed to find the best independent predictors of serum hep-25.

Variables including hep-25, hep-20, hep-25:hep-20 ratio, ferritin, CRP and creatinine were log-transformed and expressed as geometric means with 95% confidence intervals (CIs). In subjects with undetectable hep-20, the value of 0.1 was added for a correct log-transformation. Quantitative data were analyzed using the Student's t test or by analysis of variance (ANOVA) with polynomial contrasts for linear trend when indicated. Sex specific correlations between quantitative variables were assessed using Pearson's test. Qualitative data were analyzed using the chi-square test, with analysis for linear trend when indicated. Independent determinants of serum hep-20 and hep-25:hep-20 ratio were estimated by means of linear regression models, including all the variables significantly associated at univariate analysis. Two-sides P values < 0.05 were considered statistically significant.

5.2 Protein Profiling Analysis

Profiling analysis were performed using ProteinChip Data Manager Client 3.5 software, according to manufacturer protocols.

The ProteinChip SELDI analysis starts with the acquisition of the spectra of the samples. The SELDI spectrum is the graphical representation of a sample's protein profile, where each peak represent a protein or peptide component of the sample. The peak intensity is correlated to the amount of the corresponding species. Spectra selected for the same analysis must be generated at the same condition (array chemistry, stringency of binding and washing buffers, matrix, laser energy).

5.2.1 Subjects

The main clinical and biochemical characteristics of all the pool of subjects selected for the analysis are displayed in Table 1. Of note, for each pathological condition we selected an appropriate control group matched for age and sex.

Iron-Deficiency Anemia (IDA):

These subjects (n=28) were selected among the VB population, based on the presence of all the three following criteria: ferritin (Ft)<15 ng/ml, haemoglobin (Hb)<12 g/dl, mean corpuscular volume (MCV)<85 fl. For this specific IDA group, age- and sex-matched controls were selected from the whole VB dataset, providing that all the following criteria were satisfied: ferritin levels between 15 and 150 ng/ml (females) and 20-300 ng/ml (males), Hb 12-16 g/dl, MCV 86-102 fl.

Iron Overload (IO) subjects:

Subjects (n=25) with Ft>200 ng/ml (females) and Ft>300 ng/ml (males) were selected from VB database, after exclusion of subjects with any mutation on HFE gene, and without any inflammatory conditions (CRP≤0.5 mg/dl or fibrinogen<450 mg/dl). Other exclusion criteria were BMI>30 kg/m² (to avoid dysmetabolic hyperferritinemia) and Ft>700 ng/ml were excluded from the analysis because they could represent cases of obesity or non-HFE hemochromatosis respectively. Controls were age and sex matched subjects (n=25) selected with the same criteria for the controls reported above.

Myelodysplastic syndrome (MDS) subjects:

These subjects (n=24) were selected from those enrolled in another study in which our lab was involved (Santini et al., 2011). MDS subtypes, according to the WHO classification, were distributed as following: 15 patients with Refractory Anemia (RA), 8

patients with Refractory Anemia with Ringed Sideroblasts (RARS) and 1 with Chromosome 5q deletion syndrome (5q-). Sex and age matched control subjects (n=24) were selected among VB population, using the same criteria of the profiling study reported above.

Iron Refractory Iron Deficiency Anemia (IRIDA) subjects:

Spectra of 7 IRIDA subjects were selected, and 7 healthy controls were selected among VB population, with the following parameters: Ft range 15-150 ng/ml (females) and 20-300 ng/ml (males), Hb 12-16 g/dl, MCV 86-102 fl. Age- and sex-matching was not feasible in this group, since IRIDA patients were very young, so we chose the youngest subjects of VB population.

Subjects with inflammatory conditions:

Serum from subjects reporting inflammatory parameters (n=12) (CRP>100 mg/l) hospitalized in our Internal Medicine Division were collected. Non inflamed control subjects and with normal iron status (see criteria above), age and sex matched with inflamed subjects, were selected among Val Borbera database.

	N	IDA (n=28)	N	Ctrl (n=27)	p°	N	IO (n=25)	N	Ctrl (n=25)	p°	N	MDS (n=24)	N	Ctrl (n=24)	p°	N	Inflamed (n=12)	N	Ctrl (n=12)	p°
	Age (yrs)	28	48±18	27	48±18	NS	25	61±15	25	61±15	NS	24	74±10	24	73±10	NS	12	74±19	12	69±21
% males	28	7.1	27	7.4	NS [§]	25	68.0	25	72.0	NS [§]	24	70.8	24	70.8	NS [§]	12	66.7	12	50.0	NS [§]
BMI	28	24.3±3.72	27	24.8±5.45	NS	25	25.1±3.02	25	26.8±3.78	NS	-	n.a.	24	27.9±5.61	n.a.	-	n.a.	12	24.9±5.7	n.a.
Iron (µg/dl)	28	35.8±18.3	27	106±35	**	25	112±34	25	89.0±27.4	*	24	142±60	24	93.1±26.7	*	9	40.3±30.3	12	93.8±30.0	*
Tf (mg/dl)	28	328±64	27	232±32.7	**	25	227±34	25	229±31	NS	24	206±38	24	220±26	NS	9	190±62	12	249±41	*
Ft (ng/ml) [•]	28	4.85 (4.10-5.81)	27	43.4 (34.8-54.6)	**	25	340 (302-380)	25	116 (94.6-140)	**	24	503 (369-679)	24	132 (108-159)	**	9	265 (112-633)	12	66.7 (47.5-93.7)	*
Tf Sat (%) [•]	28	6.82 (5.37-8.58)	27	30.6 (25.8-36.2)	**	25	33.4 (29.1-38.5)	25	26.6 (22.9-30.6)	*	24	47.5 (38.1-59.1)	24	28.8 (25.5-32.5)	**	9	12.4 (6.69-23.3)	12	25.5 (19.7-33.1)	*
Hb (g/dl)	28	10.9±1.01	27	13.9±0.93	**	25	14.5±1.48	25	14.8±0.99	NS	24	10.6±2.04	24	14.6±1.07	**	10	12.4±1.55	12	14.6±0.83	*
hepc25 (nM) [•]	28	1.07 (0.69-1.68)	27	4.10 (2.89-5.87)	**	25	16.4 (13.1-20.9)	25	9.58 (6.62-13.9)	*	24	1.60 (0.98-2.59)	24	12.6 (10.1-15.5)	**	12	40.0 (27.1-59.1)	12	5.05 (2.66-9.58)	**
MCV (fl)	28	81.7±6.71	27	92.0±3.13	**	25	94.9±4.25	25	91.7±3.51	*	24	98.5±9.44	24	93.2±3.25	*	-	n.a.	12	92.9±4.56	n.a.
CRP (mg/dl) [•]	20	0.17 (0.12-0.24)	21	0.18 (0.13-0.30)	NS	25	0.25 (0.17-0.36)	16	0.13 (0.10-0.16)	*	24	0.11 (0.06-0.19)	24	0.15 (0.12-0.19)	NS	11	17.3 (12.1-24.8)	10	0.12 (0.09-0.14)	**

Table 1. Mean parameters and standard deviation about subjects analyzed by Protein Profiling.

°: t-test for evaluating mean value differences between each pathological group and the corresponding controls; §: χ squared test; •: log-transformed variables are shown as geometric mean with 95% confidence interval; *: p-value <0.05; **: p-value <0.001.

N: sample size; **BMI**: Body Mass Index; **Tf**: transferrin; **Ft**: ferritin; **Tf Sat**: transferrin saturation; **Hb**: haemoglobin; **hepc25**: hepcidin25; **MCV**: mean corpuscular volume; **CRP**: C-Reactive Protein; **n.a.**: not available; **NS**: not significant; **IDA**: Iron deficiency anaemia; **IO**: Iron overload; **MDS**: Myelodysplastic syndrome; **Inflamed**: Patients with inflammatory conditions.

5.2.2 Analysis

MASS CALIBRATION

A calibration equation, generated using data obtained from mass calibration standards, was applied to experimental samples (external calibration).

PROCESSING SPECTRAL DATA

The shape of the baseline in the spectra was examined and adjusted in order to subtract the noise contributions and to calculate more accurately peak intensities. When necessary, the values for the Fitting Width and Smoothing settings were adjusted according to manufacturer protocol. The default filter setting has been used for all the analysis (Average filter of 0.2 times expected peak width), that is suitable in most cases. The noise range was set with a starting mass that excluded peaks in the matrix attenuation range (usually it was set at 1600 mass value), and ended at the end of the spectrum.

PROCESSING CONDITIONS

In each analysis, the spectra were normalized by their Total Ion Current (TIC). The minimum starting mass was set at the same value of the noise range, and the end was set at 15000 mass/charge ratio (m/z) for all the analyses. Spectra were normalized, generating normalization factors which could be used to identify spectra of poor quality. The software generates a histogram displaying normalization factors; spectra outside the normal distribution were eliminated (acceptable range is 0.5-3.0). Spectrum alignment was performed for reducing mass variations of peaks within a group of spectra. Some well-resolved peaks, present in all the spectra of the same analysis, were selected within the mass range of interest. These labeled peaks within a reference spectrum were used

to create a new calibration equation for each spectrum; this resulted in higher precision between the spectra.

GENERATION AND ANALYSIS OF PEAK GROUPS

A list of all the peaks and their corresponding intensities across all the spectra was created (peak clusters) and displayed in a table. The automatic peak detection algorithm of the software was used. It labels all peaks that fulfill the specified thresholds. The main parameters for clustering are the sensitivity setting for Peak Detection and the mass window setting for Cluster Completion. To control the sensitivity with which peaks are detected for clustering, the signal-to-noise ratio (S/N), valley depth and minimum percentage of spectra in which to require peak detection, have to be specified. The automatic first-pass peak detection was set with 5 times S/N, a valley depth of 3 and a the minimum peak threshold percentage of 20%. The mass window for peak clustering was defined as 0.3% of the peak mass, suitable for low-mass range. The second-pass peak detection was set to 2 for peak S/N and 2 for valley depth. The addition of estimated peaks was done using the “autocentroid” option, which places an estimated peak using a centroid operation. The mass range for this analysis was set starting from the end of matrix attenuation, up to 15000 Da. Peaks that were not automatically placed at the appropriate peak centroid, were manually adjusted to the correct location using the cluster editing process within the software. A statistical analysis of spectra was performed in order to identify clusters that exhibit significant differences in intensity values between sample groups. The Calculated P-value function was used and peak clusters with good quality were manually inspected searching for candidate biomarkers. P-values <0.05 were considered significant. Using the function Spectrum Viewer it was

possible to check the graphic representations of cluster data, i.e. m/z mass scatter plot, group box and whiskers plot, and group scatter plot displaying average group intensities as horizontal lines. Receiver-operating characteristic (ROC) plots were automatically generated by using the P-Value Wizard, and Area Under the ROC curve (AUC) was automatically calculated. Peaks with AUC values close to 1.0 and 0.0 were considered good biomarker candidates, with high specificity and sensitivity, while a value close to 0.5 indicates that the protein expression levels completely overlapped between the groups considered. Cluster peaks could also be visualized as a heat map, showing peak clusters as green or red points with variable shades based on relative expression level.

5.2.3 Lucid Proteomics System

The Lucid Proteomics System combines SELDI's chromatographic retention technology with high performance mass spectrometry. This system provides a complete SELDI-based biomarker discovery solution that includes both protein expression profiling and identification of biomarker candidates. After the separation of serum samples onto IMAC30-Cu⁺ ProteinChip arrays, the same arrays can be loaded through a dedicated interface on mass spectrometer (Figure 5). Small peptides can be identified by direct on-array TOF/TOF analysis, while larger proteins require enrichment, purification, and digestion followed by TOF/TOF analysis (Jourdain et al., 2010).

Our protein identifications were performed using a MALDI-TOF-TOF UltrafleXtreme (Bruker Daltonics, Bremen, Germany), equipped with 1 kHz smartbeam II laser ($\lambda = 355$ nm) and operating in the positive reflectron ion mode. The instrumental conditions were: IS1 = 25 kV; IS2 = 21.65 kV; reflectron potential = 26.3 kV; delay time = 0 nsec. The matrix

was α -cyano-4-hydroxycinnamic acid (HCCA) (saturated solution in H₂O/Acetonitrile (50:50; v/v) containing 0.1% TFA). Five μ L of purified tryptic digest and 5 μ L of matrix solution were mixed and 1 μ L of the resulting mixture was deposited on the stainless steel sample holder, and allowed to dry before introduction into the mass spectrometer. External mass calibration (Peptide Calibration Standard) was based on monoisotopic values of [M+H]⁺ of Angiotensin II, Angiotensin I, Substance P, Bombesin, ACTH clip (1-17), ACTH clip (18-39), Somatostatin 28 at m/z 1046.5420, 1296.6853, 1347.7361, 1619.8230, 2093.0868, 2465.1990 and 3147.4714, respectively.

TOF/TOF experiments were performed using the LIFT device with the following experimental conditions: IS1: 7.5 kV; IS2: 6.75 kV; Lift1: 19 kV; Lift2: 3.7 kV; Reflector1: 29.5 kV; Delay time: 70 ns.

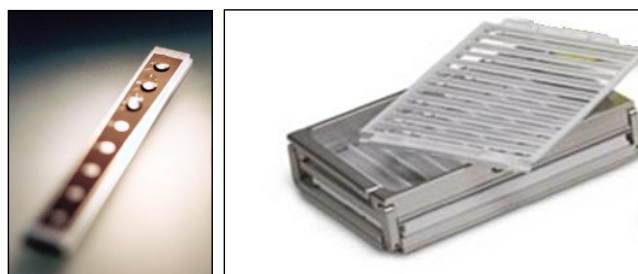


Figure 5. ProteinChip array and the dedicated adaptor of Lucid Proteomics System.

MASS SPECTROMETRIC PEPTIDE ANALYSIS

The identification of the peptides was performed through a collaboration with **The Institute of Molecular Science and Technologies (ISTM)** in Padova, by MALDI-TOF-TOF system used for Lucid System (see above).

5.3 Co-Immunoprecipitation (Co-IP) experiments

Co-IP reactions exploit the specific antigen/antibody interaction, and have the final aim to determine whether two proteins interact or not. A bait protein is precipitated with its specific antibody and then the interacting proteins are recovered.

Our bait protein was recombinant MT-2, fused with a FLAG peptide, kindly provided by our collaborators at the University Vita-Salute, San Raffaele Hospital, Milan. This tag was used to immobilize the protein onto an Anti-flag resin (ANTI-FLAG[®] M2 Agarose Affinity Gel, Sigma-Aldrich), that is a purified mouse IgG1 monoclonal antibody covalently attached to agarose by hydrazide linkage. The construct so obtained was incubated with sera samples with high levels of the SPI, in order to verify its interaction with MT-2. The whole procedure is reported below.

5.3.1 Sera samples selection

Sera of patients with low levels of the SPI (n=4) were selected among IDA subjects and the same number of patients with high levels of SPI were selected among IO and MDS subjects, according to the results obtained in protein profiling analysis. A first Western blot (for the procedure see chapter 3.3.3) was performed on these sera samples to detect the SPI, in order to confirm our hypothesis that the upregulation of its fragments corresponded to a low level of the whole protein and *viceversa*.

The total protein quantification was performed with Bicinchoninic acid (BCA) protein assay kit (Pierce Company), measuring the absorbance at 562 nm and using Bovine Serum Albumin (BSA) as protein standard for the calibration curve.

5.3.2 Co-IP protocol

After resuspension, the ANTI-FLAG resin was centrifuged at 3000g for 3 min at 4°C in order to remove the glycerol. The packed gel was then washed twice with phosphate buffer (PBS) and then incubated for 2 hrs at 4°C (shaking) with cell lysate containing MT2-flag, loading 1 mg total protein content, in 500 µl total volume of lysis buffer (200 mM Tris HCl pH 8, 1 mM EDTA, 100 mM NaCl, 10% glycerol, 0.5% NP-40, protease inhibitor). Then the resin was washed three times with lysis buffer and incubated 24 hrs at 4°C (shaking) with sera samples of interest, loading 1 mg of total protein content, reaching 500 µl total volume by adding lysis buffer. After the incubation, three washing steps were performed with lysis buffer, shaking for 15 min at 4°C each time and centrifuging at 1000 g at 4°C for 5 min. After the last wash, the resin was resuspended in sample buffer with 4% β-mercaptoethanol and boiled for 3 min. After a centrifugation step (5000 g for 30 sec), the supernatant was recovered and transferred to a fresh tube.

5.3.3 Immunoblotting analysis

Samples were separated by sodium dodecyl sulfate–polyacrylamide gel electrophoresis (SDS-PAGE), using 4% stacking and 12% running minigels (Bio-Rad) (1.5 mm spacers). Electrophoresis was carried out at 70 V until the samples entered in the running gel, and then it was set at 120 V (15 mA/gel) until the bromophenol blue front has reached the bottom of the gel. Then the proteins were transferred electrophoretically onto nitrocellulose (NC) membranes using the Mini Trans-Blot[®] Cell (Bio-Rad), setting a voltage of 100 V for 1 hr, and blocked incubating o/n with blocking buffer (Table 2). Membranes were probed with 1:1000 anti-SPI monoclonal murine primary antibody (Abnova), diluted with blocking buffer, shaking for 1 hr at room temperature (RT). After washing three

times with wash buffer (Table 2) on a rotating shaker for 15 min, the membrane was incubated with 1:5000 horseradish peroxidase-conjugated anti-mouse secondary antibody (Sigma Aldrich) diluted with blocking buffer, shaking for 1 hr at RT. After three further washing steps, the immunoblots were detected by chemiluminescence using the ECL Plus Western Blotting Detection Reagents (GE Healthcare Life Sciences) and then developing the images on Kodak BioMax XAR Films in the darkroom, adjusting the exposure time depending on the intensity of the protein bands.

<i>Running Buffer</i>
1.4% (w/v) Glycine
3% (w/v) Tris
0.1% (v/v) SDS
<i>Transfer Buffer</i>
1.4% (w/v) Glycine
3% (w/v) Tris
10% (v/v) Isopropanol
<i>10x TBS buffer (pH 7.6)</i>
6.1% (w/v) Tris
8.8% (w/v) NaCl
<i>Wash Buffer (TBS-T)</i>
0.1% (v/v) Tween 20 in 1xTBS
<i>Blocking Buffer</i>
3% (w/v) skimmed milk in 1xTBS-T
<i>Sample Buffer (4x)</i>
1M Tris, pH 6
8% (w/v) SDS
40% (v/v) Glycerol
Bromophenol Blue (one pinch)

Table 2. Immunoblot buffer solutions.

6. RESULTS and DISCUSSION

6.1 Val Borbera Project

6.1.1 Hepcidin-25 analysis in VB population

Serum hep-25 was measured by SELDI-TOF-MS in 1657 serum samples of the VB cohort, 929 females and 728 males, age range 18-98, mean age 55.4 ± 17.8 years. The age and sex distribution of this population is reported on figure 6.

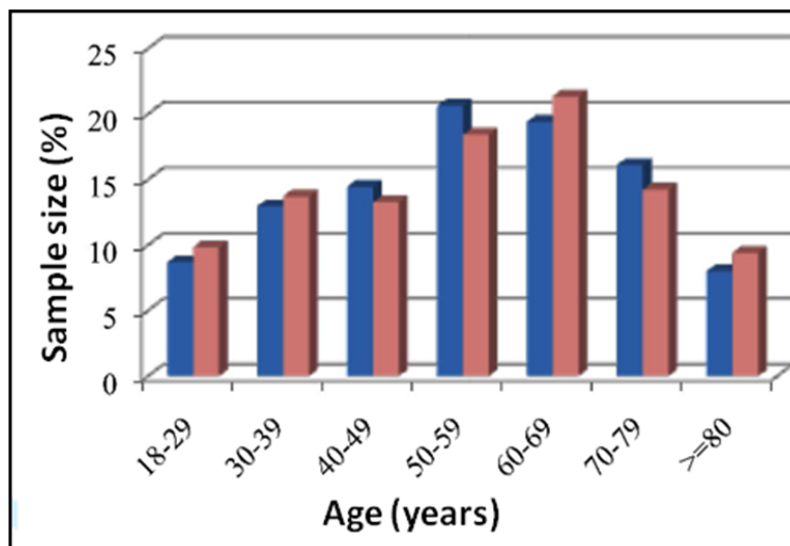


Figure 6. Age and sex distribution of the VB individuals. In blue are indicated males, in pink are shown females subjects.

Anthropometric data, red cell parameters, serum iron, transferrin, transferrin saturation and ferritin concentrations were available for all samples (Table 3). Hepcidin and ferritin showed strong age- and sex-dependent variations (Figure 7B and 7C and Table 4), and this was observed, to a lesser extent, also for transferrin saturation (Figure 7A). In males, serum hepcidin levels were rather stable across the different age groups, while in women we observed more dynamic changes.

Trait	Units	Males			Females			p°
		N	Mean	sd	N	Mean	sd	
Weight	Kg	727	78.5	12.4	927	64	12.1	****
Waist	cm	712	93	10.3	912	88	12.2	****
BMI	kg/m ²	727	26.5	3.8	926	25.5	4.8	****
Hb	g/dl	728	15.4	1.2	927	13.7	1.1	****
Hct	%	728	46	3.2	927	41.9	3	****
MCV	fl	728	91.2	4.8	927	90.6	5.1	**
MCH	pg	728	30.5	1.8	927	29.5	2	****
MCHC	%	728	33.5	1.1	927	32.6	1.2	****
Iron	µg/dl	727	105.9	36.1	925	91	30.8	****
Transferrin	mg/dl	727	235.8	36.7	925	248.2	44.9	****
Ferritin	ng/ml	726	160.7	134	923	65.1	62.7	****
Transferrin Saturation	%	727	32.3	12.1	925	26.8	10.5	****
Hepcidin°	nM	727	7.77	C.I. (7.24-8.33)	928	4.85	C.I. (4.48-5.21)	****
Hepcidin/Ferritin	pmol/µg	726	88.9	79.8	923	179.9	284.8	****
Hepcidin/Transferrin Saturation	%	727	0.39	0.5	925	0.34	0.5	*
Total Cholesterol	mg/dl	727	200.1	40.9	925	209	40.5	*
HDL cholesterol	mg/dl	727	53.4	12.6	925	63.2	14.3	****
LDL cholesterol	mg/dl	727	122.9	34.2	925	126.9	35.7	*
Tryglicerides	mg/dl	727	118.9	88.1	925	94.7	50.8	****
CRP	mg/dl	492	0.26	0.42	638	0.27	0.4	NS

Table 3. Characteristics of the VB population by sex.

°t-test for evaluating mean value differences between males and females; °log transformed variables are shown as geometric mean with 95% confidence interval.

*p <0.05, ** p <0.01, *** p <0.001, **** p <0.0005.

BMI: Body Mass Index; CRP: C-Reactive Protein; N: Sample size; sd: standard deviation; NS: not significant.

In fact, premenopausal women had hepcidin levels lower (4-5 nM) than in men of the same age (11-12 nM). In males and women aged 50-70, the hepcidin levels were similar (around 11 nM), while among the elderly, hepcidin levels decreased in both genders,

more markedly in women. Notwithstanding anemia was not the main focus of this population study, these data suggest that the hormone is unlikely to play a major role in the so called “anemia of elderly”. Ferritin levels showed a trend similar to hepcidin. Indeed, ferritin levels were quite stable in men across all age groups, while in women we observed a strict variation depending on three main age groups. Women aged 18-50 years had the lowest values, which increased in the 50-70 years interval, and then tend to decrease after the seventh decade.

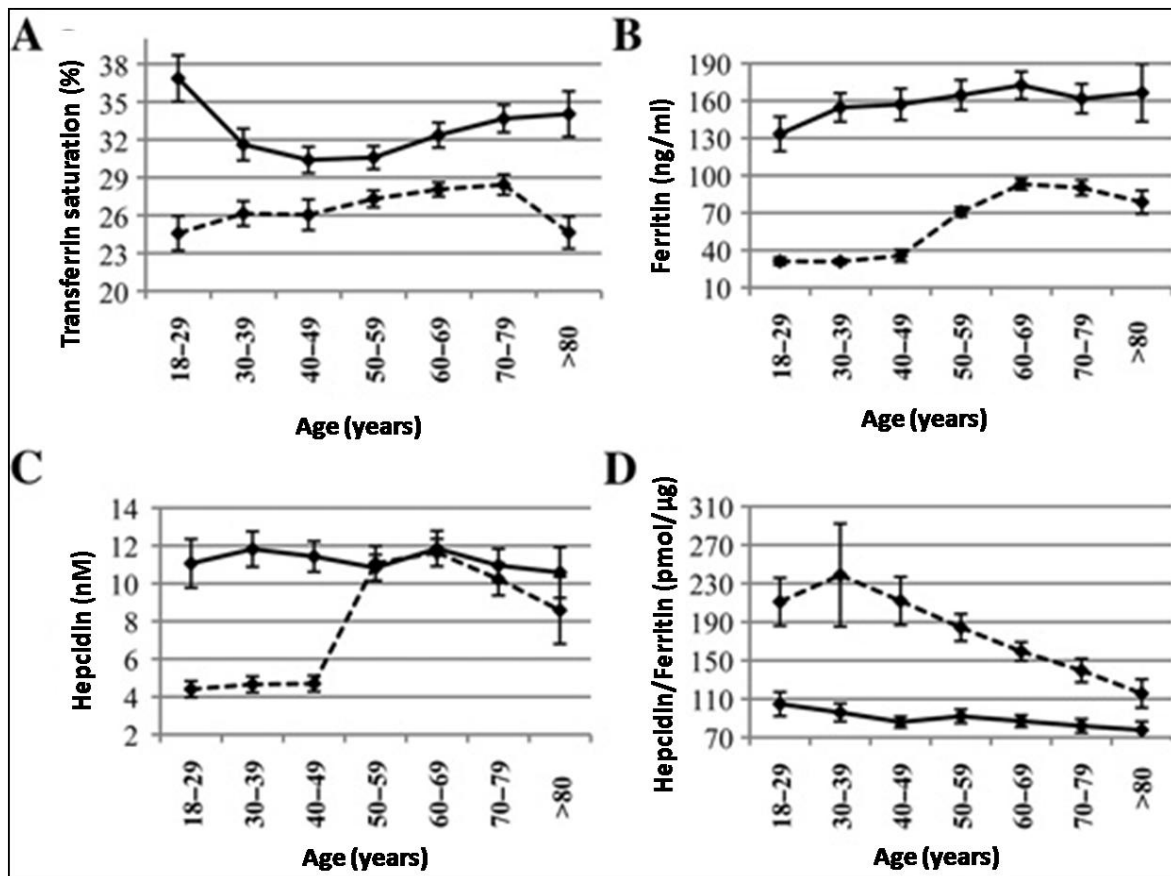


Figure 7. Age and sex dependent variations of transferrin saturation (A), serum ferritin (B), serum hepcidin (C), and hepcidin/ferritin ratio (D) in the whole population. Males are indicated by a continuous line, females by a dotted line. Bars indicate SEs.

We also considered the hepcidin/ferritin ratio (Figure 7D) to correct for hepcidin changes according to iron stores (Piperno et al., 2007, van Dijk et al., 2008). This parameter is

thought to represent the ability to increase hepcidin as a function of body iron stores. The trend represented in Figure 7D clearly remarks a large difference between young males and females, that sharply decreases with ageing. We can observe that it is higher in females, even in age groups with hepcidin levels comparable to males, indicating that the threshold for hepcidin increase in response to body iron is lower in females or that females have a greater capacity than males to modulate hepcidin as a function of iron stores.

Age class	N	Males	N	Females
18-29	63	11.1 (1.3)	91	4.4 (0.4)
30-39	94	11.8 (0.9)	127	4.7 (0.4)
40-49	105	11.4 (0.8)	123	4.7 (0.4)
50-59	150	10.8 (0.7)	171	11.1 (0.9)
60-69	141	11.8 (0.9)	198	11.6 (0.7)
70-79	117	11 (0.9)	132	10.2 (0.9)
>=80	58	10.6 (1.3)	87	8.6 (1.8)

Table 4. Serum hepcidin-25 levels by age and sex. Values are represented as means, nM; Standard errors are in brackets.

Serum hepcidin correlation analysis by sex (Table 5) yielded a significant coefficient for ferritin ($r=0.32$ and $r=0.53$ in men and women, respectively) and CRP ($r=0.25$ in women). These results confirm the known influence of iron status and inflammation on hepcidin levels. A subset of 1206 subjects was obtained excluding from the whole population subjects with iron deficiency (ferritin <30 ng/ml), inflammation (CRP values >1 mg/dl), incomplete information, and subjects with undetectable hepcidin caused by multiple causes like blood donation, advanced age (>80 year old), β -thalassaemia trait or heavy alcohol intake (>80 g/die for men, >40 g/die for women).

Trait	Males	Females
Weight	-0.0238	0.1064*
Waist	0.0156	0.1736*
BMI	0.0065	0.1558*
Hb	-0.0792*	0.1050*
Hct	-0.0741*	0.1278*
MCV	0.0338	0.0856*
MCH	0.0143	0.0554
MCHC	-0.0226	-0.0227
Iron	0.0307	0.1090*
Transferrin	-0.1781*	-0.1784*
Ferritin	0.3194*	0.5263*
Transferrin saturation	0.0742*	0.1472*
Triglycerides	0.0353	0.1588*
CRP	0.0851*	0.2512*

Table 5. Sex specific correlation analysis of serum hepcidin-25.
 * Pearson's r significantly different from zero at the p<0.05 level
BMI: Body Mass Index; **CRP:** C-Reactive Protein.

Linear regression analysis were performed on this subset of subjects, using log transformed hepcidin and age as covariate. Significant variables were tested in multiple regression models (Table 6).

Trait	Males		Females	
	β	p	β	p
Age	-0.0048	**	0.043	****
Squared age	-	NS	-0.0004	****
Ferritin	0.9918	****	0.0036	****
Hb	-0.0669	**	-	NS
MCHC	-0.0923	****	-	NS
Total cholesterol	-	NS	0.0018	**

Table 6. Multiple regression analysis of serum hepcidin by sex.
 *p<0.05; **p<0.01; ***p<0.001; ****p<0.0005.
 Hb, haemoglobin; MCHC, mean corpuscular haemoglobin concentration.

Age, ferritin, Hb and mean corpuscular haemoglobin concentration (MCHC) resulted independent predictors of hepcidin levels in males and accounted for 13.5% of the total hepcidin variability. In females, age, ferritin and total cholesterol were the independent predictors, accounting for 17.7% of its variability. The population was stratified in three classes according to serum ferritin levels, corresponding to iron deficiency (Ft <30 ng/ml), normal iron balance (30 ng/ml ≤ Ft ≤200 ng/ml in females and 30 ng/ml ≤ Ft ≤300 ng/ml in males) and iron overload (Ft >200 ng/ml in females and Ft >300 ng/ml in males). Mean hepcidin levels increased progressively with Ft increasing and differed significantly among the three groups (p<0.001) (Figure 8A). This trend reflects the response of hepcidin to iron stores and confirms the result of serum ferritin as a predictor of hepcidin levels. Grouping the population according to transferrin saturation no significant differences in hepcidin levels were observed (Figure 8B).

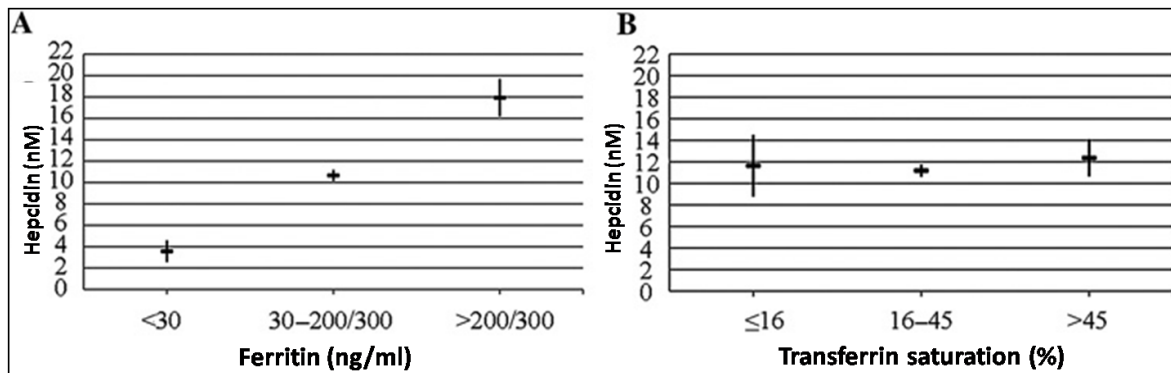


Figure 8. Serum hepcidin in groups of individuals classified according to their serum ferritin levels (A) and transferrin saturation (Tf Sat) (B). Three classes are shown: iron deficiency (ferritin < 30ng/ml and Tf Sat≤16%), normal iron status (intermediate values) and iron overload (ferritin > 200 ng/ml in females and > 300 ng/ml in males and Tf Sat>45%). Mean values are age- and sex-adjusted by ANOVA (95% C.I.).

In summary, all the data here presented reveal a strong correlation of serum hepcidin with serum ferritin, an index of tissue iron, in both sexes, confirming results previously observed in a small number of individuals (Kroot et al., 2009, Piperno et al., 2011), but

not with circulating iron, represented by serum iron, transferrin and transferrin saturation. So in steady conditions at population level, hepcidin appears mainly determined by iron stores.

6.1.2 *Hepcidin-20 analysis in VB population*

Serum levels of hep-20 were measured in the cohort of VB population, taking advantage from the spectra obtained for hep-25 determination by SELDI-TOF-MS. Hep-20 was detectable in 854 out of 1577 (54.2%) subjects, at variance with hep-25, which was detectable in 89.1% of subjects. Subjects with detectable hep-20 were older and had higher body iron status (as reflected by transferrin saturation and ferritin levels) and hep-25 levels as compared to subjects with undetectable hep-20 (Table 7).

	Hepcidin-20 undetectable	Hepcidin-20 detectable	<i>P</i>
	N=723	N=854	
Male sex (%)	40	48.8	<0.001
Age (years)	53.0 ± 17.8	58.0 ± 17.6	<0.001
BMI	25.6 ± 4.2	26.3 ± 4.6	0.001
s-iron (µg/dl)	96.19 ± 35.91	98.49 ± 32.51	0.246
Transferrin (mg/dl)	247.75 ± 44.79	237.23 ± 37.90	<0.001
Transferrin Saturation %	28.52 ± 12.12	29.95 ± 11.14	0.015
Ferritin* (ng/ml)	52 (48-57)	86 (81-92)	<0.001
Hb (g/dl)	14.4 ± 1.4	14.5 ± 1.4	0.039
CRP* (mg/l)	0.16(0.15-0.17)	0.17(0.16-0.18)	0.225
Creatinine* (µmol/l)	0.83(0.82-0.85)	0.87(0.85-0.88)	0.001
Hep-25* (nmol/l)**	3.11 (2.72-3.56)	7.36 (6.83-7.94)	<0.001
Hep-25* (nmol/l)***	7.05 (6.60-7.54)	8.48 (8.04-8.94)	<0.001

Table 7. Main characteristics of subjects stratified according to hepcidin-20 detectable.

*: variables not normally distributed are expressed as geometric means with 95% CIs. **: geometric mean of hep-20 and hep-25 with 95% CIs calculated on whole population (1577 subjects). ***: geometric mean of hep-25 with 95% CIs calculated on 1405 subjects (with hep-25 detectable).

The two hepcidin isoforms were significantly and positively correlated in both sexes (males: $r=0.48$, $P<0.001$; females: $r=0.45$, $P<0.001$; Figure 9). At univariate analyses, hep-20 also significantly correlated with age, hemoglobin, and CRP in men, and with age, body mass index (BMI), ferritin, CRP and creatinine in women (Table 8). At multivariate linear regression analysis hep-25 and age resulted as independent significant predictors of hep-20 in men. In women, hep-25, age, BMI, and ferritin were the independent predictors of hep-20 (Table 9A and B). In figure 10A and 10B respectively, the variations of hep-20 in the VB population according to different ranges of age and iron status (ferritin levels) are reported.

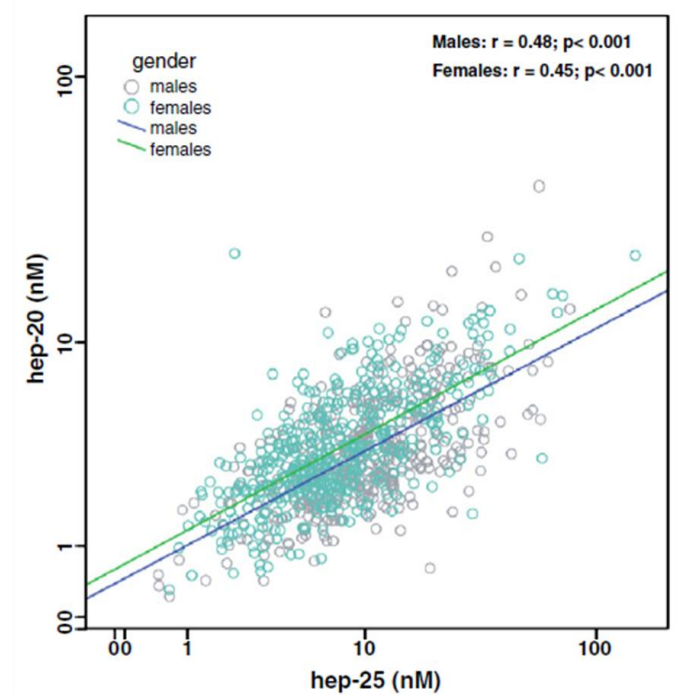


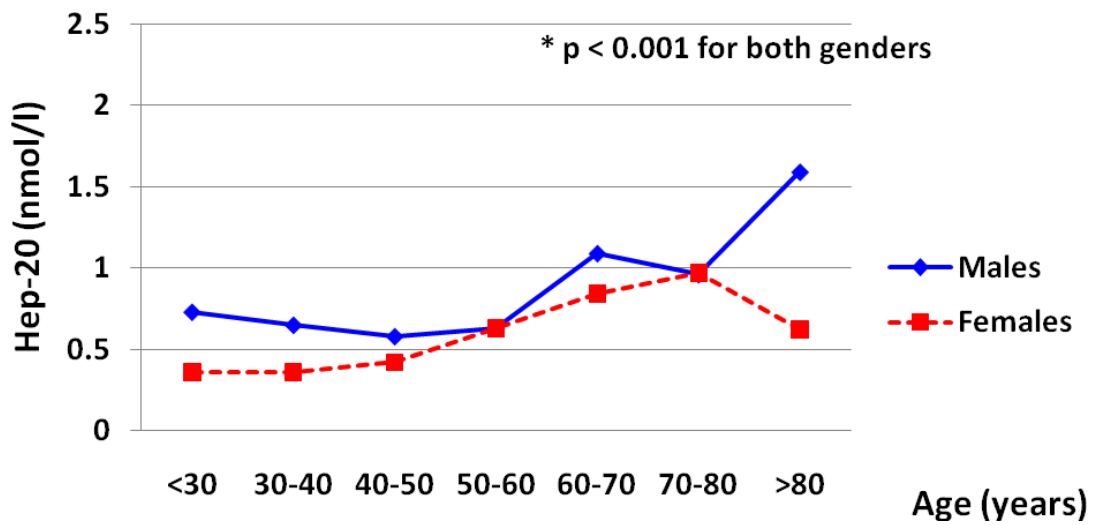
Figure 9. Correlation plot between hep-20 and hep-25 (logarithmic scale).

Trait	Males		Females	
	Correlation	p	Correlation	p
Hep-25 (nmol/l)	0.480	<0.001	0.449	<0.001
Age (years)	0.096	0.049	0.178	<0.001
BMI	0.049	0.315	0.186	<0.001
s-iron (µg/dl)	-0.028	0.571	-0.023	0.627
Transferrin (mg/dl)	-0.039	0.430	-0.049	0.308
Transferrin saturation %	-0.005	0.912	-0.013	0.789
Ferritin ^a (ng/ml)	0.062	0.206	0.149	0.002
Hb (g/dl)	-0.110	0.024	-0.048	0.320
CRP ^a (mg/l)	0.115	0.052	0.173	0.002
Creatinine ^a (µmol/l)	-0.028	0.583	0.109	0.029

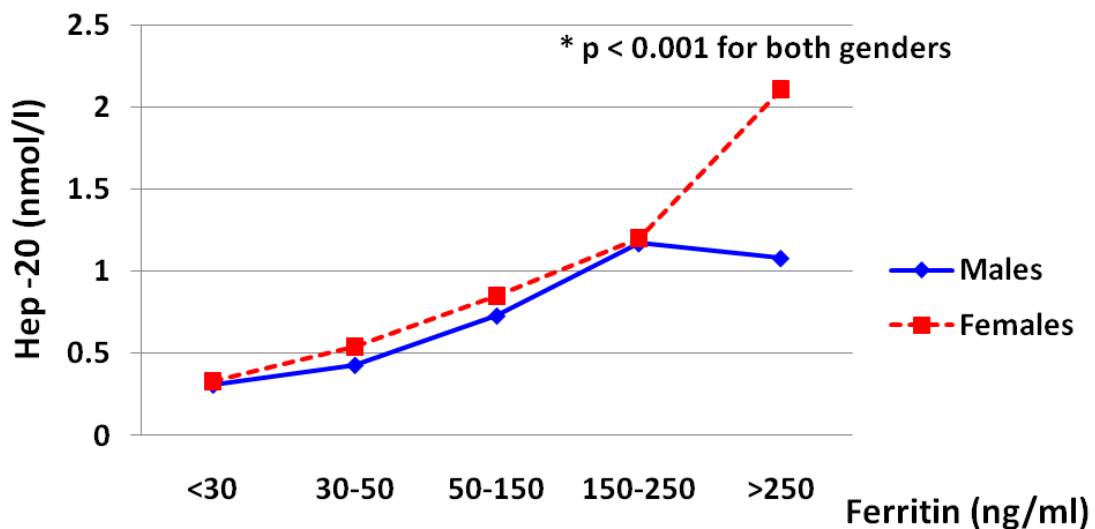
Table 8. Sex specific correlation analysis of hep-20. Values in bold are those considered statistically significant (P<0.05). * Variables not normally distributed are expressed as geometric means with 95% CIs.

A		
	Males	
	β-coefficient	P
Hep-25 (nmol/l)	0.627	<0.001
Age (years)	0.126	0.007
B		
	Females	
	β-coefficient	P
Hep-25 (nmol/l)	0.553	<0.001
Age (years)	0.177	0.004
Ferritin (µg/l)	-0.255	0.001
BMI	0.163	0.003

Table 9. Predictors of hep-20 levels in males (A) and females (B).



Hep-20 (nmol/l) Males	0.73 (0.45-0.85)	0.65 (0.44-0.94)	0.58 (0.41-0.82)	0.63 (0.47-0.84)	1.09 (0.81-1.48)	0.96 (0.67-1.36)	1.59 (1.03-2.44)
Hep-20 (nmol/l) Females	0.36 (0.25-0.52)	0.36 (0.26-0.48)	0.42 (0.30-0.57)	0.63 (0.47-0.85)	0.84 (0.64-1.09)	0.97 (0.70-1.34)	0.62 (0.41-0.92)



Hep-20 (nmol/l) Males	0.31 (0.18-0.52)	0.43 (0.24-0.78)	0.73 (0.61-0.89)	1.17 (0.90-1.53)	1.08 (0.77-1.51)
Hep-20 (nmol/l) Females	0.33 (0.27-0.40)	0.54 (0.41-0.71)	0.85 (0.70-1.03)	1.20 (0.77-1.87)	2.11 (0.68-6.53)

Figure 10. Behavior of hep-20 in VB population according to different ranges of age (A) and ferritin (B), respectively. Males are indicated by continuous blue line, females by a red dotted line. * by ANOVA with polynomial contrasts for linear trend

In figure 11, hep-20 and hep-25 levels are also reported in parallel, after stratification for ferritin levels. Then the hep-25:hep-20 ratio was considered, particularly in relation to age and iron parameters of VB subjects (Table 10 and 11).

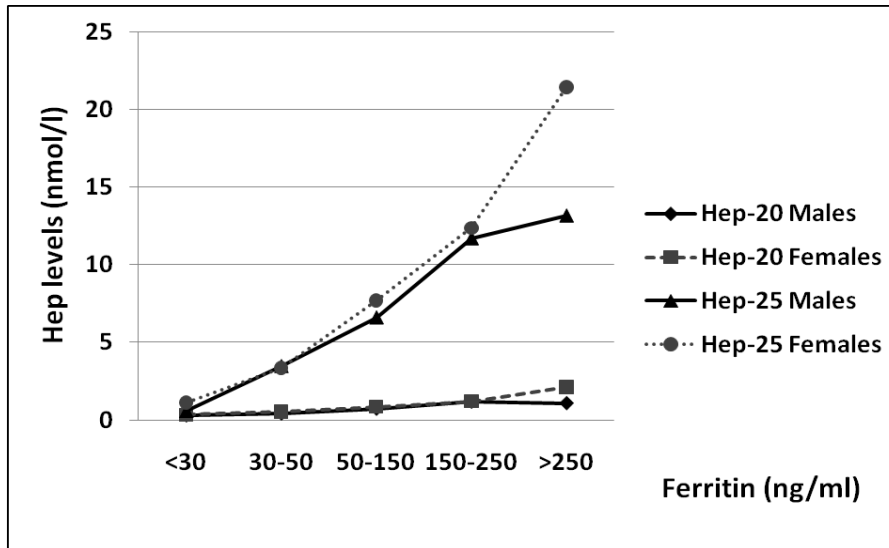


Figure 11. Behaviour of hep-20 and hep-25 according to iron status.

Trait	Males		Females	
	Correlation	p	Correlation	p
Age (years)	-0.119	0.015	0.136	0.006
BMI	-0.027	0.588	0.073	0.137
s-iron (µg/dl)	0.098	0.046	0.118	0.016
Transferrin (mg/dl)	-0.074	0.135	-0.193	<0.001
Transferrin saturation %	0.106	0.032	0.172	<0.001
Ferritin ^a (ng/ml)	0.497	<0.001	0.564	<0.001
Hb (g/dl)	-0.009	0.850	0.134	0.006
CRP ^a (mg/l)	0.043	0.472	0.063	0.284
Creatinine ^a (µmol/l)	-0.061	0.234	0.037	0.470

Table 10. Sex specific correlation analysis of hep-25:hep-20 ratio.

* Variables not normally distributed are expressed as geometric means with 95% CIs.

	Males		Females	
	β -coefficient	P	β -coefficient	P
Ferritin ($\mu\text{g/l}$)	0.504	<0.001	0.662	<0.001
Age (years)	-0.147	0.001	-0.198	<0.001

Table 11. Predictors of hep-25:hep-20 ratio in males and females.

This analysis was done just in subjects with both hepcidin isoforms detectable (n=824). The hep-25:hep-20 ratio was lower in premenopausal women than in males of the same age (within 50 years old), and this difference decreased in the older age groups (Figure 12A). In figure 12B the trend of hep-25:hep-20 ratio according to ferritin levels is reported, showing a progressive increase with increasing iron stores. In figure 13 the relative percentages of hep-25 and hep-20 are reported, according to increasing ferritin levels in males (A) and in females (B) respectively. The relative percentage of hep-20 progressively and significantly decreased with increased ferritin levels, in both sexes.

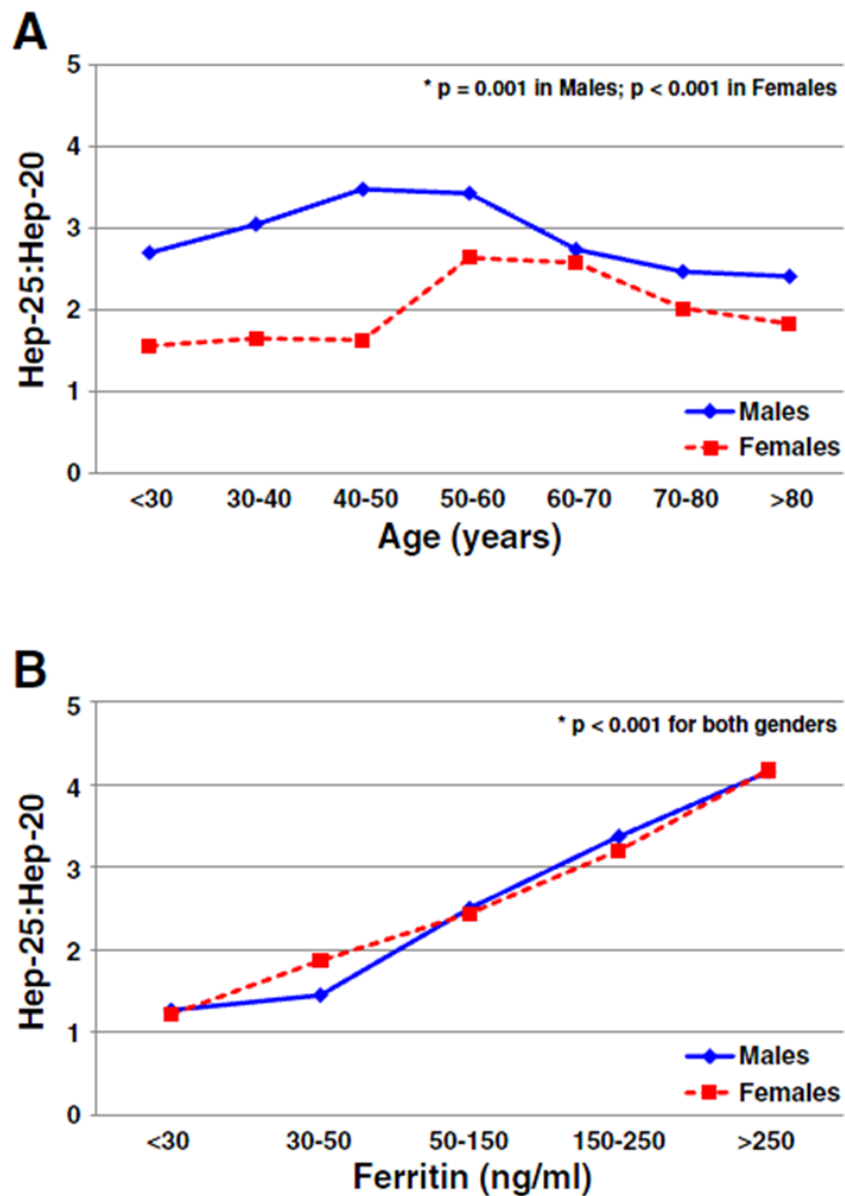


Figure 12. Hep-25:hep-20 ratio in groups of individuals classified according to age (A) and ferritin levels (B), respectively. Males are indicated by blue continuous line, females by a red dotted line. * by ANOVA with polynomial contrasts for linear trend.

Taken together, the results of the present study suggest that the relative contribute of hep-20 to total serum hepcidin is not negligible at population level. In the total population, mean hep-20 levels were about 14% of corresponding hep-25 levels, and when considering only subjects with detectable hep-25 levels (n=1405) this percentage increased up to 42.1%.

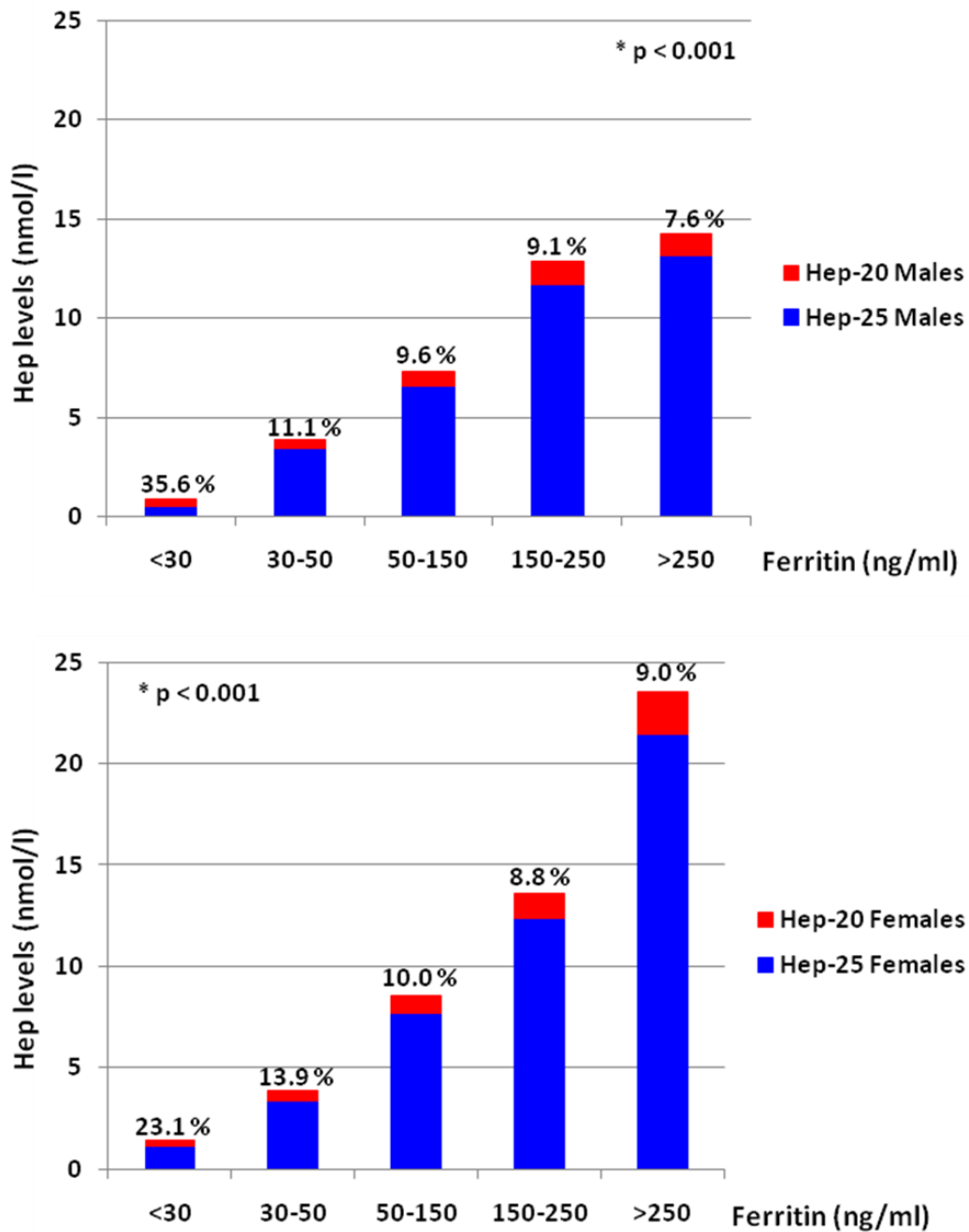


Figure 13. Relative percentages of hep-25 and hep-20 according to increasing ferritin levels in males (A) and females (B), respectively. The percentage value over the column represents the proportion of hep-20 on total hep (calculated as hep-20+hep-25). * by ANOVA with polynomial contrasts for linear trend.

Until now the origin and the biological meaning of the two hep-20 and hep-22 isoforms are still unknown, and so it is unclear whether or not the processing of hep-25 cleavage is an actively regulated mechanism. Hep-20 could represent either a final inactive

degradation byproduct of hep-25 or a functional peptide whose production is actively regulated. Recent studies highlighting the relevant antimicrobial properties of hep-20 (Maisetta et al., 2010, Tavanti et al., 2011), as well as pilot studies about its increased concentration in several diseases (Campostrini et al., 2010, Peters et al., 2010, Suzuki et al., 2009, Tomosugi et al., 2006), may support the latter hypothesis. The results here presented, particularly those about hep-25:hep-20 ratio, may reinforce the same hypothesis, indicating a putative active regulation of hep-20 production. Indeed, a relative stable hep-25:hep-20 ratio would be expected in case of a simple degradation product. Remarkably, ferritin resulted an independent predictor of hep-20 in women, with a negative coefficient, and not positive as it would be expected in case of hep-20 as a mere constitutive byproduct of hep-25 degradation (Table 10). So we can speculate that in subjects with iron deficiency, an efficient degradation of hep-25, helps to keep its levels as low as possible in order to maximize intestinal iron absorption. In subjects with adequate or high iron levels hep-25 degradation is a less efficient process, in order to keep a normal iron balance or to prevent iron overload.

6.2 Profiling Analysis

The Protein Profiling analysis performed on the different subsets of subjects affected by iron homeostasis disorders in comparison to sex and age matched controls, resulted in a list of peptides with some corresponding information, like mass, peak intensity, statistical information (p-value and ROC area).

Iron Deficiency Anaemia Profiling

Iron deficiency anemia (IDA) is the most common nutritional deficiency in the world (Clark, 2008), causing up to 50% of anemia (Worldwide prevalence of anemia 1993-2005, WHO Global Database on Anaemia, 2008). IDA occurs in up to 11% of women aged 20-49 years and 2-4% of men over 50 years (Looker et al., 1997). These data are in accordance with the cases of the disease, found among VB subjects and selected for our analyses. Indeed, 22 out of 28 IDA subjects were premenopausal women (aged 21-49 years). This group also included 4 post-menopausal women (80-92 years old), and 2 men (52 and 65 years old).

IDA is generally caused by a negative iron balance that limits hemoglobin synthesis in erythrocyte precursors (Ganz and Nemeth, 2012, Liu and Kaffes, 2012). The main causes of a negative iron balance are an inadequate iron intake, an impaired absorption, or loss of iron due to various conditions like menses or gastrointestinal bleeding.

Among the VB population we selected subjects affected by IDA, according to the criteria described in Materials and Methods section, and a corresponding set of control subjects (age and sex matched). The spectra of these two experimental groups were analysed by ProteinChip Data Manager Software for comparative proteomic analysis. In the following

table, modulated peaks resulting from the analysis are reported (each m/z value corresponds to a peptide/protein) (Table 12).

average m/z	p-value	ROC area	average m/z	p-value	ROC area
2789	4.29E-05	0.18	3683	1.21E-02	0.72
3480	1.38E-03	0.75	2360	1.33E-02	0.70
3159	2.18E-03	0.72	3263	1.33E-02	0.69
2601	2.88E-03	0.75	2866	1.40E-02	0.69
3291	2.88E-03	0.72	10080	1.40E-02	0.69
6848	2.88E-03	0.76	4283	1.46E-02	0.67
2030	3.22E-03	0.72	4486	1.61E-02	0.69
3818	3.58E-03	0.73	4504	1.61E-02	0.69
4162	3.99E-03	0.69	2727	1.68E-02	0.70
2231	4.21E-03	0.72	4183	1.76E-02	0.66
2741.7	5.47E-03	0.75	3973	1.84E-02	0.69
2143	5.76E-03	0.70	3168	2.30E-02	0.69
3340	7.07E-03	0.72	3363	2.63E-02	0.69
1988	7.43E-03	0.70	3129	2.74E-02	0.67
3275	7.43E-03	0.69	3310	2.86E-02	0.67
4020	8.21E-03	0.69	2013	2.99E-02	0.63
2883	1.00E-02	0.70	3957	2.99E-02	0.65
2083	1.05E-02	0.69	4095	3.25E-02	0.67
3144	1.16E-02	0.69	2630	3.68E-02	0.65
4299	1.16E-02	0.69	3774	3.84E-02	0.67

Table 12. Modulated Peaks obtained comparing spectra from IDA patients to spectra from healthy controls (positive group for ROC: IDA subjects).

The most significantly modulated peak, i.e. downregulated with p-value=4.29E-05, ROC=0.18 (see Table 12 and Figure 14) had a mass of 2789.7 which matched the mass of hep-25. We could confirm this “identification” by using our synthetic standard of hep-25. As already mentioned, hepcidin, the key peptide hormone involved in iron homeostasis, inhibits iron entry into plasma from the three main sources of iron: dietary absorption in the duodenum, the release of recycled iron from macrophages and the release of iron stored in hepatocytes (Ganz and Nemeth, 2012). Iron is one of the main regulators of

hepcidin production, so that when iron is abundant more hepcidin is produced by hepatocytes, blocking intestinal iron absorption and release from stores and macrophages. In case of iron deficiency, less hepcidin is produced in order to allow entry of iron in the plasma compartment. So in IDA patients we observed the expected downregulation of hepcidin, as shown in figure 14.

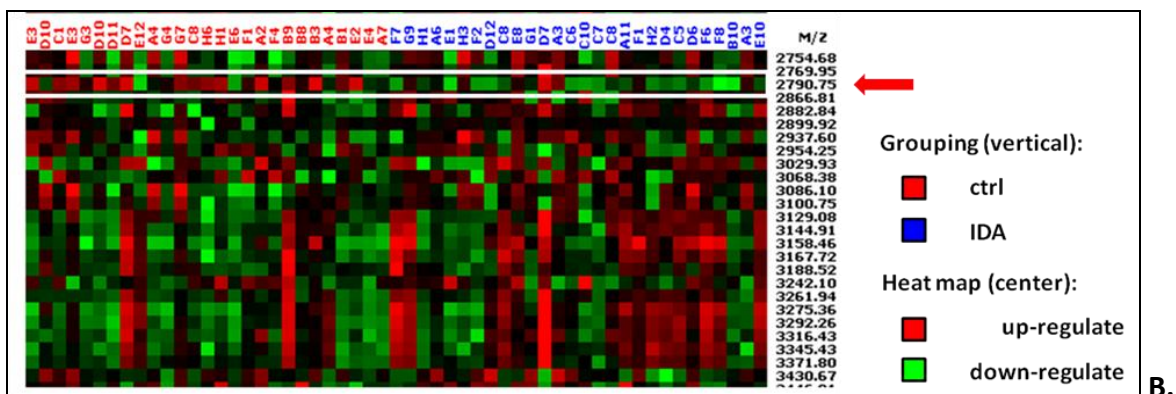
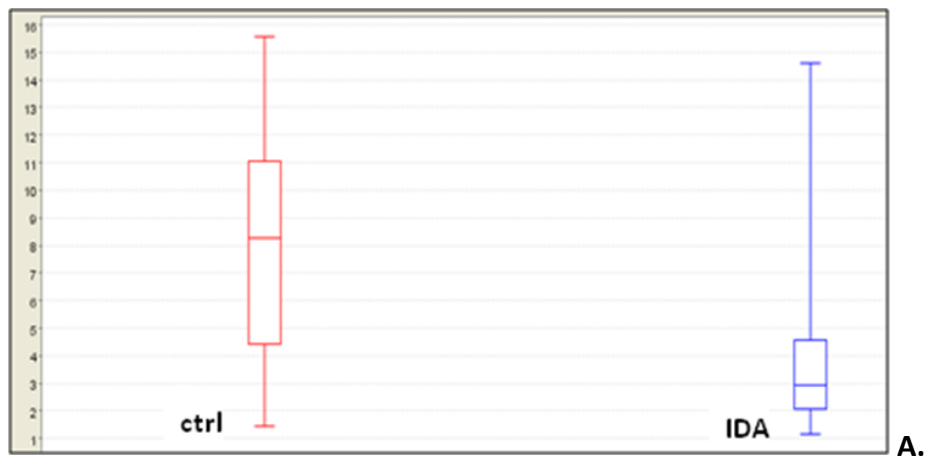


Figure 14. Hecpidin as main modulated peak in the profiling of IDA patients. A. whisker plot representing hepcidin distribution in the two subgroups; **B.** Heat map profile of some peptides modulated in IDA patients. Hecpidin profile is indicated by the red arrow: its down-regulation in subjects with iron deficiency anemia is shown by green dots, while the up-regulation in controls by red dots.

Regarding the other modulated peaks, we performed a literature survey to check whether some other studies had been already conducted on them. The literature search of mass values returned a few studies regarding some peptides derived from the

fragmentation of a larger protein, which was a putative SPI, a plasma glycoprotein with a molecular weight of 120 kDa, mainly expressed in the liver, acting as an acute-phase protein in several species. Interestingly, some of these peptides were previously reported by Chen and colleagues (Chen et al., 2010) as significantly upregulated in myelodysplastic patients compared to controls (peaks at m/z 3274, m/z 3956, m/z 3972, m/z 4282 and m/z 4298). The authors identified these peaks by liquid chromatography–tandem mass spectrometry (LC/MS-MS). In another paper by Clarke et al. (Clarke et al., 2011), the authors searched for new markers for the detection of early stage epithelial ovarian cancer. The list of peptides included a cleavage fragment of SPI (average mass at 3273 Da) as well Peng and colleagues (Peng et al., 2009) identified by mass spectrometry 21 peaks commonly observed in serum samples loaded on SELDI ProteinChip and notably, among those peaks, five (average mass at 1532 Da, 2029 Da, 2273 Da, 3159 Da and 4283 Da) were identified as derived from SPI fragmentation. Moreover Zhang et al. found the m/z 3272 peptide as a possible biomarker of early stage ovarian cancer (Zhang et al., 2004). Song and colleagues characterized the fragmentation of human serum SPI and demonstrated its association with different disease conditions (diabetes and several cancers including ovarian, breast, colon, prostate and pancreatic) (Song et al., 2006). The authors measured the relative abundance of the fragments within the so called proline-rich region (PRR), and some of them have similar mass to peptides resulted differentially expressed in our profiling analyses, like peaks at mass 4283, 3956, 3273, 3141 and 2724 Da. In our protein profiling analyses on IDA patients we observed a significant upregulation of the majority of the putative SPI fragments compared to corresponding controls (Table 13).

m/z	REGULATION in IDA	p-value	ROC area
3158	up-regulated	2.18E-03	0.72
3275	up-regulated	7.43E-03	0.69
3956	up-regulated	2.99E-02	0.65
3972	up-regulated	1.84E-02	0.69
4282	up-regulated	1.46E-02	0.67
4298	up-regulated	1.16E-02	0.69
3142	up-regulated	1.20E-02	0.69
3028	up-regulated	n.s.	/
2881	up-regulated	9.00E-03	0.70
2724	up-regulated	1.00E-02	0.70
2627	up-regulated	3.70E-02	0.65
2570	up-regulated	n.s.	/
2471	down-regulated	n.s.	/
2358	up-regulated	1.30E-02	0.70
2271	up-regulated	n.s.	/

Table 13. List of putative SPI fragments and their regulation in IDA profiling analysis (ROC area calculated considering IDA patients the positive group). n.s.= not statistically significant (p-value>0.05).

Iron Overload Profiling

Several conditions can lead to iron accumulation in the liver. Iron overload can be genetically determined but, in many other cases, non genetic iron loading factors are present (Pietrangelo et al., 2011). The most common iron overload disorder is HFE-hereditary haemochromatosis (HH) (Siah et al., 2006), characterized by a genetic defect disrupting a protein involved in the positive regulation of hepcidin. Other, “non-HFE” genetic hemochromatosis are caused by pathogenic mutations in other genes involved in hepcidin regulation like transferrin receptor 2 (*TFR2*), hemojuvelin (*HJV*), or hepcidin itself (*HAMP*), or its receptor ferroportin (*FPN*) (Pietrangelo et al., 2011).

For the selection of our iron overloaded subjects, we decided to exclude those with any HFE mutation or with ferritin levels higher than 700 ng/ml, to avoid the inclusion of subjects with HFE or “non-HFE” hemochromatosis. We also excluded obese subjects or

subjects with inflammation, since both these conditions are known to interfere with iron metabolism, stimulating hepcidin production (Martinelli et al., 2012, Pietrangelo et al., 2007, Verga Falzacappa et al., 2007, Wrighting and Andrews, 2006).

Table 14 reports the differentially expressed peaks in iron overloaded subjects as compared with subjects with normal iron stores.

average m/z	p-value	ROC area
12447	4.81E-05	0.80
12608	5.33E-04	0.77
2791	7.63E-03	0.71
8932	1.07E-02	0.74
3159	1.66E-02	0.29
13231	1.66E-02	0.32
1782	2.26E-02	0.31
2754	3.05E-02	0.34
3972	3.05E-02	0.32
4298	3.05E-02	0.34
5804	3.20E-02	0.34
3774	3.70E-02	0.32
2143	4.46E-02	0.31
2727	4.46E-02	0.32
13565	5.12E-02	0.34

Table 14. Modulated Peaks resulted by comparing iron overload patients to healthy controls (positive group for ROC: iron overload subjects).

As mentioned above, iron is a positive regulator of hepcidin production, through both liver iron stores and circulating transferrin-bound iron (Tf-Fe₂). In iron overloaded subjects we observed an highly significant (p-value= 7.63E⁻³) increase of hepcidin peak (m/z 2790.6). High levels of hepcidin decrease plasma iron concentration, blocking iron intestinal uptake and its export from enterocytes and macrophages.

Of note, the analysis of the other peaks, showed that some of the putative SPI fragments reported in the previous profiling analysis of IDA subjects, resulted again significantly modulated in IO subjects, but with an opposite direction, as indicated in table 15. In

particular four peaks, i.e. m/z 3158, 3972, 4298 and 2724, were downregulated in iron overload conditions compared to control subjects. Four peaks (m/z 3275, 3956, 4282 and 3027.6) had the same trend but didn't reach the significance.

m/z	REGULATION in IO	p-value	ROC area
3158	down-regulated	1.66E-02	0.29
3275	down-regulated	n.s.	0.34
3956	down-regulated	n.s.	0.356
3972	down-regulated	3.05E-02	0.32
4282	down-regulated	n.s.	0.34
4298	down-regulated	3.05E-02	0.34
3142	n.d.	/	/
3028	down-regulated	n.s.	0.39
2881	n.d.	/	/
2724	down-regulated	4.46E-02	0.32
2627	n.d.	/	/
2570	n.d.	/	/
2471	n.d.	/	/
2358	n.d.	/	/
2271	n.d.	/	/

Table 15. List of putative SPI fragments and their regulation in IO profiling analysis (ROC area calculated with iron overload patients as positive group). **n.s.**= not statistically significant (p-value>0.05); **n.d.**= not determined, peaks not detected in the spectra.

Myelodysplastic syndromes (MDS) Profiling

Myelodysplastic syndromes (MDSs) are a heterogeneous group of haematopoietic malignancies characterized by ineffective haemopoiesis, blood cytopenia and a hypercellular bone marrow (Chen et al., 2010). Patients often undergo blood transfusions, substantially contributing to iron overload in MDS.

Table 16 reports all peaks modulated in our MDS subjects compared to healthy controls. MDS subjects had high average ferritin levels compared to controls (632 ng/ml vs 144 ng/ml respectively), and higher transferrin saturation (53.9% vs 30% respectively) (see Table 1-C), indicating iron overload.

average m/z	p-value	ROC area
12626	3.26E-09	0.02
13373	4.74E-09	0.03
12457	4.14E-08	0.06
11361	8.27E-08	0.06
11748	9.27E-08	0.08
14702	2.83E-07	0.09
11954	3.16E-07	0.08
4074	4.87E-07	0.91
4444	1.91E-06	0.13
7978	1.91E-06	0.91
4134	2.11E-06	0.11
8356	2.34E-06	0.89
5623	2.59E-06	0.89
5874	3.86E-06	0.14
6674	3.86E-06	0.88
5910	6.95E-06	0.14
7935	1.02E-05	0.89
8146	1.02E-05	0.88
14130	1.49E-05	0.14
8944	1.64E-05	0.16
9301	1.80E-05	0.14
5072	2.37E-05	0.14

average m/z	p-value	ROC area
13902	4.45E-05	0.17
6116	6.90E-05	0.17
7771	8.94E-05	0.86
7572	1.15E-04	0.81
13591	1.36E-04	0.20
11103	3.33E-04	0.19
6483	4.93E-04	0.81
3976	9.01E-04	0.23
2956	9.70E-04	0.23
9150	1.12E-03	0.23
6645	1.21E-03	0.77
3887	1.30E-03	0.77
5342	1.85E-03	0.26
4687	1.98E-03	0.77
6850	1.98E-03	0.75
3277	2.12E-03	0.26
10675	2.61E-03	0.27
4286	3.19E-03	0.27
9507	8.31E-03	0.29
3161	9.95E-03	0.72
3961	9.95E-03	0.33
4302	1.33E-02	0.28

Table 16. List of peaks modulated in MDS patients compared to healthy subjects (positive group for ROC: MDS subjects).

Despite this, in our profiling analysis, hepcidin resulted downregulated in MDS subjects compared to controls, with average concentration of 2.82 nM vs 14.30 nM respectively, although this modulation doesn't reach the statistical significance (p -value=0.08). A trend toward hepcidin downregulation, despite high levels of circulating iron, could be explained by the ineffective erythropoiesis, that counteracts the opposite regulation mediated by iron. This is in accordance with a previous study by our group in a large cohort of MDS patients stratified according to different World Health Organization (WHO) subtypes (Santini et al., 2011). We showed that the erythropoietic stimulus tends to prevail in RA, 5q- syndrome and particularly in RARS, with a relatively blunted response to

iron as indicated by hepcidin/ferritin ratio, similarly to what we observed in the MDS subjects selected for this study.

Regarding the regulation of the putative SPI fragments, we found that the same fragments reported by Chen et al. (Chen et al., 2010), i.e. peaks with m/z 3275, 3956, 3972, 4282, 4298 and one at m/z 3158 cited by Peng et al. (Peng et al., 2009) were differentially expressed at statistically significant level. In particular, the first 5 peaks resulted significantly downregulated in the MDS subjects, while the m/z 3158 peak was upregulated compared to healthy controls. So the SPI fragments in MDS showed the same trend observed in iron overload, except for the latter peak. The other smaller peaks were not detected in the spectra used for our analysis. Table 17 shows the trend observed for the SPI fragments along with the corresponding p and ROC values.

m/z	REGULATION in MDS	p-value	ROC area
3158	up-regulated	9.95E-03	0.72
3275	down-regulated	2.12E-03	0.26
3956	down-regulated	9.95E-03	0.33
3972	down-regulated	9.01E-04	0.23
4282	down-regulated	3.19E-03	0.27
4298	down-regulated	1.33E-02	0.28
3142	n.d.	/	/
3028	n.d.	/	/
2881	n.d.	/	/
2724	up-regulated	n.s.	/
2627	n.d.	/	/
2570	n.d.	/	/
2471	n.d.	/	/
2358	n.d.	/	/
2271	n.d.	/	/

Table 17. List of putative SPI fragments and their regulation in MDS profiling analysis (ROC area calculated considering MDS patients the positive group). **n.s.**= not statistically significant (p-value>0.05); **n.d.**= not determined, peaks not detected in the spectra.

Iron Refractory Iron Deficiency Anemia (IRIDA) Profiling

IRIDA is a rare hereditary recessive anemia caused by a mutation in the gene encoding for Matriptase-2 (MT-2), a transmembrane serin protease mainly expressed in the liver, acting as a negative regulator of hepcidin. It cleaves cell surface HJV (mHJV), a protein that behaves as coreceptor of BMPs, impairing hepcidin expression (Silvestri et al., 2008). This activity depends on the integrity of its protease domain.

As consequence, subjects affected by IRIDA are characterized by anemia, low transferrin saturation and inappropriately high serum hepcidin levels for the low iron status. Moreover, they are generally refractory to oral iron treatment (De Falco et al., 2013). The list of modulated peaks resulting from our comparative analysis between IRIDA patients and healthy controls is reported in table 18.

We noticed a highly significant upregulation of hepcidin in IRIDA patients (p -value= $2.70E^{-3}$). Moreover, among the putative SPI fragments, peaks with m/z 3972, 4282 and 4298 resulted significantly down-regulated in IRIDA subjects. Peaks at m/z 3275 and 3956 showed the same trend but without reaching the statistical significance, and all the other smaller fragments were not detectable from the spectra, probably due to the low spectra resolution. A summary of all putative SPI fragments in IRIDA (including trend and p value) is reported in table 19. It has to be mentioned that we evaluated only a limited number of subjects per experimental group ($n=7$), so a more representative pool of subjects should be enrolled for a further profiling study. Another limitation of this analysis lies on the fact that control subjects were not age matched with diseased patients, since the latter were young children and we could not find any subject of the same age among our pool of controls.

average m/z	p-value	ROC area	average m/z	p-value	ROC area
2797	2.70E-03	1.00	3323	6.64E-03	0.95
3495	2.70E-03	1.00	5813	6.64E-03	0.06
5347	2.70E-03	0.01	6492	6.64E-03	0.95
8156	2.70E-03	0.01	2584	1.01E-02	0.90
8625	2.70E-03	1.00	4302	1.01E-02	0.06
9161	2.70E-03	0.01	4477	1.01E-02	0.06
9704	2.70E-03	1.00	4288	1.52E-02	0.11
12636	2.70E-03	0.01	5909	1.52E-02	0.11
3451	4.27E-03	0.95	6121	1.52E-02	0.11
3718	4.27E-03	0.95	9311	3.21E-02	0.14
4646	4.27E-03	0.01	11760	3.21E-02	0.14
5078	4.27E-03	0.01	3379	4.55E-02	0.81
8952	4.27E-03	0.01	3979	4.55E-02	0.15
2681	6.64E-03	0.95			

Table 18. List of peaks modulated in IRIDA patients compared to healthy subjects (positive group for ROC: IRIDA subjects).

m/z	REGULATION in IRIDA	p-value	ROC area
3158	n.d.	/	/
3275	down-regulated	n.s.	0.25
3956	down-regulated	n.s.	0.19
3972	down-regulated	4.60E-02	0.15
4282	down-regulated	1.50E-02	0.11
4298	down-regulated	1.00E-02	0.06
3142	n.d.	/	/
3028	n.d.	/	/
2881	n.d.	/	/
2724	n.d.	/	/
2627	n.d.	/	/
2570	n.d.	/	/
2471	n.d.	/	/
2358	n.d.	/	/
2271	n.d.	/	/

Table 19. List of putative SPI fragments and their regulation in IRIDA profiling analysis (ROC area calculated considering IRIDA patients the positive group). **n.s.**= not statistically significant (p-value>0.05); **n.d.**= not determined, peaks not detected in the spectra.

Profiling in subjects with inflammatory conditions

Spectra of subjects with high C Reactive Protein (CRP) levels (average CRP=200 mg/L) were compared to spectra of control subjects, resulting in the differentially expressed

peaks listed below (Table 20). In our analysis the second most significantly modulated peak was hepcidin, in particular it resulted upregulated in patients with inflammation (p-value=5.31E⁻⁵). This trend is expected since inflammation is one of the known regulatory pathways of hepcidin expression, mediated by inflammatory cytokines and other microbial molecules (Ganz, 2011). It has been proved that IL-6 is necessary and sufficient for hepcidin induction during inflammation and that IL-6-hepcidin axis is responsible for the hypoferremia of inflammation (Nemeth et al., 2004). The positive effect of the cytokine on hepcidin is at transcriptional level (Nemeth et al., 2004) and it is mediated by STAT3 (Pietrangelo et al., 2007, Verga Falzacappa et al., 2007, Wrighting et al., 2006), interacting with a STAT3-binding element in the hepcidin promoter. Inflammatory disorders as well as other diseases like chronic infections, hematological malignancies and solid tumors, are characterized by a mild-to-moderate anemia and hypoferremia (the so-called “anemia of chronic disease”). High levels of hepcidin are in fact responsible for the degradation of the iron exporter ferroportin on the cell membrane of enterocytes and macrophages, determining its trapping into these cells (Ganz, 2011). The consequent iron restriction impairs the synthesis of hemoglobin.

On the other hand, regarding the modulation of the putative SPI fragments, no significant regulation resulted from our analysis of patients with inflammation compared to not inflamed controls. Since SPI is an acute phase protein (Pineiro et al., 1999), we expected a modulation of its fragments, due to the fact that either there is a large amount of this protein which need to be degraded or in case the fragmentation is needed to produce active fragments. On the base of the above consideration we checked the sera of inflamed patients for the presence of the whole SPI protein (with a band at Mr of 120

kDa) by Western blotting (see chapter 3), obtaining a strong evidence of the abundance of the unprocessed protein.

average m/z	p-value	ROC area	average m/z	p-value	ROC area
2439	3.23E-05	1.00	3890	5.58E-03	0.17
2793	5.31E-05	0.97	6113	7.91E-03	0.83
11101	5.31E-05	0.97	8146	9.37E-03	0.22
6641	6.78E-05	0.03	2866	1.30E-02	0.78
6439	1.75E-04	0.06	5812	1.30E-02	0.81
4470	5.32E-04	0.08	3244	1.53E-02	0.81
12625	1.22E-03	0.14	14136	1.53E-02	0.22
8943	1.50E-03	0.11	4073	2.09E-02	0.78
5072	1.82E-03	0.14	2027	3.27E-02	0.25
6845	2.68E-03	0.14	13377	3.27E-02	0.25
9148	3.23E-03	0.17	2676	3.77E-02	0.78
2195	4.67E-03	0.83	12985	4.33E-02	0.72
5263	4.67E-03	0.83	2275	4.96E-02	0.28
11356	4.67E-03	0.83	4798	4.96E-02	0.28

Table 20. List of differentially expressed peptides in patients with inflammation as compared to controls.

6.2.1 SPI fragments – Identification and speculations

The putative SPI fragments were analyzed through a collaboration with the IMST in Padua using MALDI-TOF-TOF analysis, as mentioned above. Only two of the several peaks were successfully identified, i.e. those at m/z 2724 and 3275. Both were recognized as fragments of SPI, confirming what we had anticipated on the basis of the literature survey. For other four peptides, i.e. those at m/z 3956, m/z 3972, m/z 4282 and m/z 4298, we can reasonably assume the identity as SPI fragments based on the similarity of the mass and also of the experimental conditions reported in the paper by Chen and colleagues (Chen et al., 2010), where they were definitively identified. The peaks at m/z 3972 and 4298 are likely the corresponding oxidized form of peptides m/z 3956 and 4282 respectively, since the mass is shifted of 16 Da (i.e. the mass of oxygen). Of note, the fragment patterns were quite similar to those reported in the previous papers,

notwithstanding the differences in the assay conditions and in sample preprocessing, thus suggesting that the observed fragmentation occurred mainly *in vivo* and not *ex vivo* (Song et al., 2006). Indeed, the final fragments pattern could be the result of a complex interplay, disease specific, between endoproteases (e.g. kallikrein) and exoproteases (e.g. carboxipeptidases and aminopeptidases).

Overall, the modulation of the putative SPI fragments in subjects with different disorders of iron homeostasis were interesting. In particular, the five peptides with m/z value of 3275, 3956, 3972, 4282 and 4298 showed an opposite trend of expression in the analysis of IDA and IO subjects. In IDA subjects they were significantly upregulated, while in iron overload they were downregulated (although the statistical significance was not invariably reached). These five peaks were also modulated in two other disorders of iron homeostasis, MDS and IRIDA. In both conditions the fragments were downregulated, although in IRIDA the peaks at m/z 3275 and 3956 did not reach the statistical significance. Taken together, the high degree of modulation of these fragments in different iron disorders suggested a possible involvement of SPI in iron metabolism. To this purpose, it should be recalled that at present the molecular mechanisms accounting for the negative regulation of hepcidin by MT2 are mainly still unknown. MT2 is a serin protease, which could theoretically represent a substrate for the SPI identified by our experiments. Of note, both MT2 and SPI proteins are highly expressed in the liver. Some preliminary experiments of coimmunoprecipitation involving recombinant FLAG-tagged MT2 and recombinant SPI performed by our collaborators at the San Raffaele Hospital in Milan provided evidences of an interaction between the two proteins. Since the conditions of these preliminary experiments were a little bit forced, we decided to

reproduce the experiment in more physiological conditions, i.e. by immunoprecipitating recombinant MT2-flag with an anti-flag resin followed by an incubation with serum samples having high SPI levels (see results in chapter 6.3).

6.2.2 Bioinformatics analysis

The molecular interaction between MT2 and SPI was also evaluated by bioinformatic analysis conducted in collaboration with Dr. Alejandro Giorgetti and Dr. Stefano Piccoli, at the Department of Biotechnology of University of Verona. They at first performed a structural and functional characterization of both proteins. Two different structural models were built for MT2 and two individual models for of the VIT and vWA domains of SPI. They tried to analyze the binding capability of SPI by MT2, by using a bioinformatic tool that predicts the likelihood of interaction of each aminoacid in a given sequence, called WHISCY (de Vries et al., 2006). Remarkably, we observed a high interaction probability for VIT domain, involving the residue arginine (Arg) 47, that is clearly exposed to the solvent. The subsequent docking simulation analysis were done considering a polypeptide containing that aminoacid of interest that was extracted from the SPI sequence and was tested for the interaction with MT2 trypsin domain models. This polypeptide was predicted to form a complex with MT2. In particular, it reached an H bond distance with aspartate (Asp) 756, entering correctly in the binding cavity. This result was observed for both the MT2 models considered in docking analysis (Figure 15 and 16).

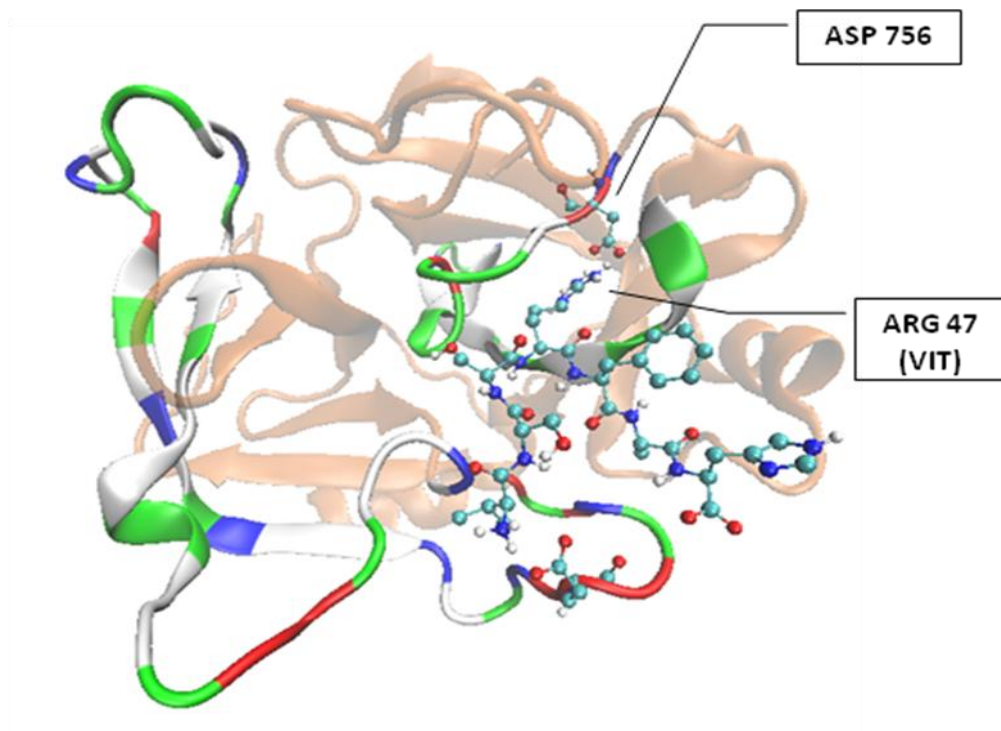


Figure 15. Protein complex of trypsin domain of matriptase 2 (1EAX as template, ribbon representation) and SPI polypeptide (ball and stick representation). The binding cavity is indicated as polarization colors.

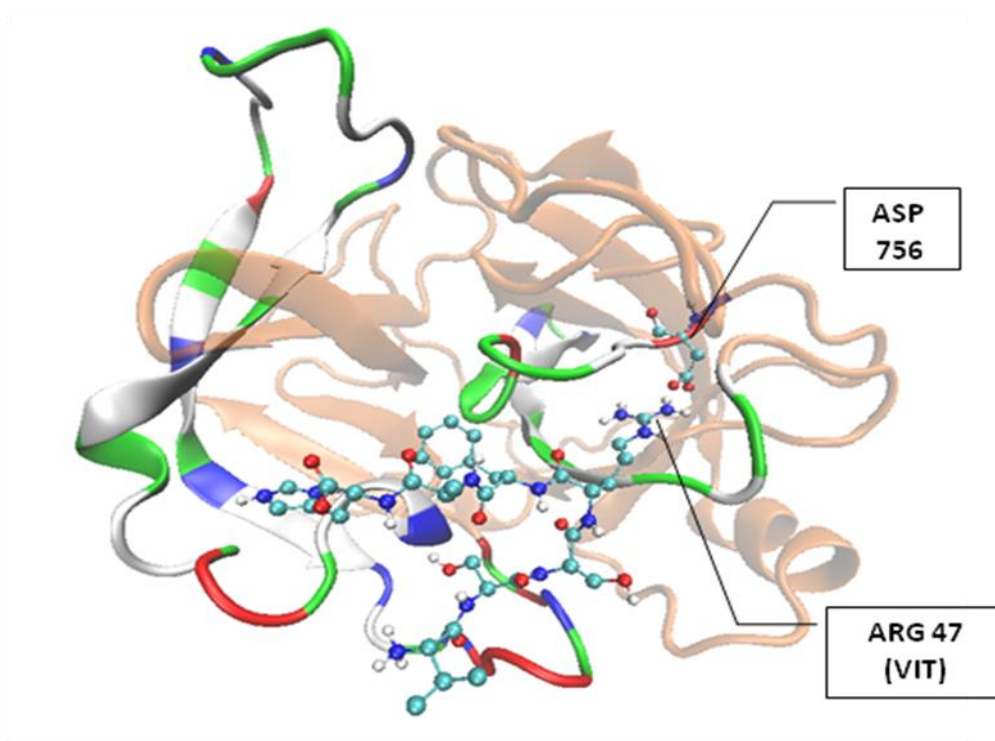


Figure 16. Protein complex of trypsin domain of matriptase 2 (4DJZ as template, ribbon representation) and SPI polypeptide (ball and stick representation). The binding cavity is indicated as polarization colors.

6.3 Co-IP experiments

In order to select serum samples with high levels of SPI to be used in the co-IP experiment, we assumed that they would correspond to the ones in which SPI fragments were found downregulated, i.e. iron overload, myelodysplastic and IRIDA patients. In the figure below (Figure 17) we can see some serum samples representative of all the samples analyzed by Western blot for SPI detection, using a primary antibody recognizing the N-terminus of the protein. In figure 17 it is possible to appreciate an inverse correlation between the abundance of the whole protein (band at 120 kDa) and its fragments (85 kDa and 57 kDa) (see Figure 4 for SPI fragmentation pattern).

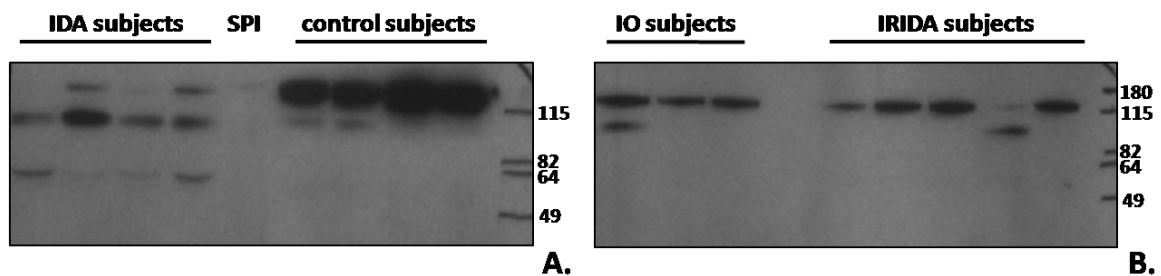


Figure 17. Western blot analysis of SPI in the sera of iron deficiency anaemia (IDA) and control subjects in **panel A**, and iron overload (IO) and Iron Refractory Iron Deficiency Anaemia (IRIDA) in **panel B**. Lower levels of SPI (120 kDa) correspond to higher levels of 85 kDa and 57 kDa fragments (IDA subjects). This trend confirms the upregulation of fragments observed in the same subjects with protein profiling analysis. (Values of the molecular weight marker are indicated in kDa). 25µg total protein were loaded per lane.

Thus we selected, for the co-IP, serum samples with high levels of SPI according to the intensity of the 120 kDa band, and we incubated them with a resin coupled to the second protein of interest, MT2. In a first experiment we managed to elute from the resin a protein at the same molecular weight of the recombinant SPI used as positive control (Figure 18).

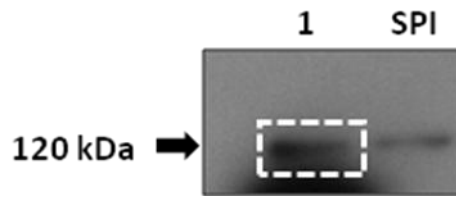


Figure 18. In **lane 1** a band corresponding to the recombinant SPI has been detected in the eluate from the MT2/resin complex.

Several experiments were subsequently performed, improving the elution steps as well as standardizing the sample application and handling. We then decided to use another anti-SPI antibody, able to detect the C-terminus of the protein, to test its presence in the eluate of the antFLAG resin. We performed a sort of positive control by using the recombinant SPI and the resin-bound MT2. In figure 19 it is possible to note a band corresponding to the positive control eluted from the MT2-coupled resin after incubation with recombinant SPI. This last experiment confirmed the results obtained by our collaborators in Milan and further strengthen the hypothesis of an interaction occurring *in vivo* between these two proteins in the peculiar setting of iron homeostasis in the body.

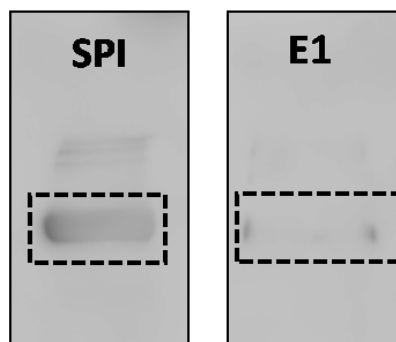


Figure 19. **SPI:** recombinant SPI (positive control); **E1:** eluate from MT2/resin complex after incubation with recombinant SPI.

7. CONCLUSIONS

Hepcidin-25 was measured in the large cohort of VB population by SELDI-TOF-MS and a valid reference range was established. This range resulted strongly age- and gender-dependent and should be taken in consideration when interpreting individual data in both research and clinical setting. The correlation analyses clearly showed that baseline hepcidin levels at population level are mainly determined by body iron stores instead of plasma iron pool. Based on our data, a major involvement of hepcidin in determining the so called “anemia of elderly” appears unlikely, since we observed a decrease (rather than an increase) of the hormone levels among subjects older than 80 years. By using the same proteomic approach, we were also able to measure hepcidin-20 at population level for the first time. This study showed that the contribution of this peptide to total serum hepcidin is not negligible at population level, and suggested an active regulation of hepcidin-25 degradation according to iron need. Spectra acquired by mass spectrometry were also used for protein profiling analysis of subset of patients affected by different disorders at the opposite end of the spectrum of iron homeostasis disorders, i.e. IDA and non genetically determined IO. These analyses allowed the identification of a common putative biomarker. Because of its molecular characterization as a putative Serin Protease Inhibitor (SPI), we could hypothesize the involvement of this molecule in the negative regulation of hepcidin expression. Subsequent experiments allowed a better characterization of SPI as a putative ligand of MT2. Our hypothesis was supported by immunoblotting experiments on real serum samples, by *in vitro* (cell lines models) experiments performed in collaboration with researchers at the San Raffaele Vita-Salute University in Milan, and by *in silico* bioinformatics analysis performed in collaboration

with researchers at the Department of Biotechnology of the University of Verona. Our working hypothesis is now under definitive confirmation through a mouse model (SPI ko mice).

REFERENCES

- Adamsky K., Weizer O., Amariglio N., Breda L., Harmelin A., Rivella S., Rachmilewitz E. and Rechavi G., Decreased hepcidin mRNA expression in thalassemic mice. *Br J Haematol* 2004; 124 (1): 123-4.
- Andrews N. C., Disorders of iron metabolism. *N Engl J Med* 1999; 341 (26): 1986-95.
- Babitt J. L., Huang F. W., Wrighting D. M., Xia Y., Sidis Y., Samad T. A., Campagna J. A., Chung R. T., Schneyer A. L., Woolf C. J., Andrews N. C. and Lin H. Y., Bone morphogenetic protein signaling by hemojuvelin regulates hepcidin expression. *Nat Genet* 2006; 38 (5): 531-9.
- Camaschella C., BMP6 orchestrates iron metabolism. *Nat Genet* 2009; 41 (4): 386-388
- Campostrini N., Castagna A., Zaninotto F., Bedogna V., Tessitore N., Poli A., Martinelli N., Lupo A., Olivieri O. and Girelli D., Evaluation of hepcidin isoforms in hemodialysis patients by a proteomic approach based on SELDI-TOF MS. *J Biomed Biotechnol* 2010; 2010 329646.
- Campostrini N., Traglia M., Martinelli N., Corbella M., Cocca M., Manna D., Castagna A., Masciullo C., Silvestri L., Olivieri O., Toniolo P., Camaschella C. and Girelli D., Serum levels of the hepcidin-20 isoform in a large general population: The Val Borbera study. *J Proteomics* 2012; 76 Spec No.:28-35.
- Caputo E., Lombardi M. L., Luongo V., Moharram R., Tornatore P., Pirozzi G., Guardiola J. and Martin B. M., Peptide profiling in epithelial tumor plasma by the emerging proteomic techniques. *J Chromatogr B Analyt Technol Biomed Life Sci* 2005; 819 (1): 59-66.
- Castagna A., Campostrini N., Zaninotto F. and Girelli D., Hepcidin assay in serum by SELDI-TOF-MS and other approaches. *J Proteomics* 2010; 73: 527-536.
- Chen C., Bowen D. T., Giagounidis A. A., Schlegelberger B., Haase S. and Wright E. G., Identification of disease- and therapy-associated proteome changes in the sera of patients with myelodysplastic syndromes and del(5q). *Leukemia* 2010; 24 (11): 1875-84.
- Choi-Miura N. H., Sano Y., Oda E., Nakano Y., Tobe T., Yanagishita T., Taniyama M., Katagiri T. and Tomita M., Purification and characterization of a novel glycoprotein which has significant homology to heavy chains of inter-alpha-trypsin inhibitor family from human plasma. *J Biochem* 1995; 117 (2): 400-7.
- Clark S. F., Iron deficiency anemia. *Nutr Clin Pract* 2008; 23 (2): 128-41.
- Clarke C. H., Yip C., Badgwell D., Fung E. T., Coombes K. R., Zhang Z., Lu K. H. and Bast R. C., Jr., Proteomic biomarkers apolipoprotein A1, truncated transthyretin and connective tissue activating protein III enhance the sensitivity of CA125 for detecting early stage epithelial ovarian cancer. *Gynecol Oncol* 2011; 122 (3): 548-53.
- Cravatt B. F., Simon G. M. and Yates J. R., 3rd, The biological impact of mass-spectrometry-based proteomics. *Nature* 2007; 450 (7172): 991-1000.
- De Falco L., Sanchez M., Silvestri L., Kannengiesser C., Muckenthaler M. U., Iolascon A., Gouya L., Camaschella C. and Beaumont C., Iron refractory iron deficiency anemia. *Haematologica* 2013; 98 (6): 845-53.
- de Vries S. J., van Dijk A. D. and Bonvin A. M., WHISCY: what information does surface conservation yield? Application to data-driven docking. *Proteins* 2006; 63 (3): 479-89.
- Flanagan J. M., Truksa J., Peng H., Lee P. and Beutler E., In vivo imaging of hepcidin promoter stimulation by iron and inflammation. *Blood Cells Mol Dis* 2007; 38 (3): 253-7.

Fung E. T., Yip T. T., Lomas L., Wang Z., Yip C., Meng X. Y., Lin S., Zhang F., Zhang Z., Chan D. W. and Weinberger S. R., Classification of cancer types by measuring variants of host response proteins using SELDI serum assays. *Int J Cancer* 2005; 115 (5): 783-9.

Ganz T., Heparin and iron regulation, 10 years later. *Blood* 2011; 117 (17): 4425-33.

Ganz T. and Nemeth E., Heparin and iron homeostasis. *Biochim Biophys Acta* 2012; 1823 (9): 1434-43.

Hentze M. W., Muckenthaler M. U., Galy B. and Camaschella C., Two to tango: regulation of Mammalian iron metabolism. *Cell* 2010; 142 (1): 24-38.

Hunter H. N., Fulton D. B., Ganz T. and Vogel H. J., The solution structure of human hepcidin, a peptide hormone with antimicrobial activity that is involved in iron uptake and hereditary hemochromatosis. *J Biol Chem* 2002; 277 (40): 37597-603.

Issaq H. J., Veenstra T. D., Conrads T. P. and Felschow D., The SELDI-TOF MS approach to proteomics: protein profiling and biomarker identification. *Biochem Biophys Res Commun* 2002; 292 (3): 587-92.

Jourdain S., Bulman A. and Dalmaso E., The Lucid Proteomics System for top-down biomarker research. *Arch Physiol Biochem* 2010; 116 (4-5): 158-62.

Kemna E., Tjalsma H., Laarakkers C., Nemeth E., Willems H. and Swinkels D., Novel urine hepcidin assay by mass spectrometry. *Blood* 2005; 106 (9): 3268-70.

Kemna E. H., Tjalsma H., Podust V. N. and Swinkels D. W., Mass spectrometry-based hepcidin measurements in serum and urine: analytical aspects and clinical implications. *Clin Chem* 2007; 53 (4): 620-8.

Koomen J. M., Shih L. N., Coombes K. R., Li D., Xiao L. C., Fidler I. J., Abbruzzese J. L. and Kobayashi R., Plasma protein profiling for diagnosis of pancreatic cancer reveals the presence of host response proteins. *Clin Cancer Res* 2005; 11 (3): 1110-8.

Kroot J. J., Hendriks J. C., Laarakkers C. M., Klaver S. M., Kemna E. H., Tjalsma H. and Swinkels D. W., (Pre)analytical imprecision, between-subject variability, and daily variations in serum and urine hepcidin: implications for clinical studies. *Anal Biochem* 2009; 389 (2): 124-9.

Kroot J. J., Laarakkers C. M., Geurts-Moespot A. J., Grebenchtchikov N., Pickkers P., van Ede A. E., Peters H. P., van Dongen-Lases E., Wetzels J. F., Sweep F. C., Tjalsma H. and Swinkels D. W., Immunochemical and mass-spectrometry-based serum hepcidin assays for iron metabolism disorders. *Clin Chem* 2010; 56 (10): 1570-9.

Kroot J. J., Tjalsma H., Fleming R. E. and Swinkels D. W., Heparin in human iron disorders: diagnostic implications. *Clin Chem* 2011; 57 (12): 1650-69.

Liu K. and Kaffes A. J., Iron deficiency anaemia: a review of diagnosis, investigation and management. *Eur J Gastroenterol Hepatol* 2012; 24 (2): 109-16.

Looker A. C., Dallman P. R., Carroll M. D., Gunter E. W. and Johnson C. L., Prevalence of iron deficiency in the United States. *JAMA* 1997; 277 (12): 973-6.

Maisetta G., Petruzzelli R., Brancatisano F. L., Esin S., Vitali A., Campa M. and Batoni G., Antimicrobial activity of human hepcidin 20 and 25 against clinically relevant bacterial strains: effect of copper and acidic pH. *Peptides* 2010; 31 (11): 1995-2002.

Martinelli N., Traglia M., Campostrini N., Biino G., Corbella M., Sala C., Busti F., Masciullo C., Manna D., Previtali S., Castagna A., Pistis G., Olivieri O., Toniolo D., Camaschella C. and Girelli D., Increased serum

hepcidin levels in subjects with the metabolic syndrome: a population study. *PLoS One* 2012; 7 (10): e48250.

Miyamae T., Malehorn D. E., Lemster B., Mori M., Imagawa T., Yokota S., Bigbee W. L., Welsh M., Klarskov K., Nishimoto N., Vallejo A. N. and Hirsch R., Serum protein profile in systemic-onset juvenile idiopathic arthritis differentiates response versus nonresponse to therapy. *Arthritis Res Ther* 2005; 7 (4): R746-55.

Nemeth E., Rivera S., Gabayan V., Keller C., Taudorf S., Pedersen B. K. and Ganz T., IL-6 mediates hypoferremia of inflammation by inducing the synthesis of the iron regulatory hormone hepcidin. *J Clin Invest* 2004; 113 (9): 1271-6.

Nemeth E., Tuttle M. S., Powelson J., Vaughn M. B., Donovan A., Ward D. M., Ganz T. and Kaplan J., Hepcidin regulates cellular iron efflux by binding to ferroportin and inducing its internalization. *Science* 2004; 306 (5704): 2090-3.

Nemeth E., Preza G. C., Jung C. L., Kaplan J., Waring A. J. and Ganz T., The N-terminus of hepcidin is essential for its interaction with ferroportin: structure-function study. *Blood* 2006; 107 (1): 328-33.

Nishimura H., Kakizaki I., Muta T., Sasaki N., Pu P. X., Yamashita T. and Nagasawa S., cDNA and deduced amino acid sequence of human PK-120, a plasma kallikrein-sensitive glycoprotein. *FEBS Lett* 1995; 357 (2): 207-11.

Papanikolaou G., Samuels M. E., Ludwig E. H., MacDonald M. L., Franchini P. L., Dube M. P., Andres L., MacFarlane J., Sakellaropoulos N., Politou M., Nemeth E., Thompson J., Risler J. K., Zaborowska C., Babakaiff R., Radomski C. C., Pape T. D., Davidas O., Christakis J., Brissot P., Lockitch G., Ganz T., Hayden M. R. and Goldberg Y. P., Mutations in HFE2 cause iron overload in chromosome 1q-linked juvenile hemochromatosis. *Nat Genet* 2004; 36 (1): 77-82.

Papanikolaou G., Tzilianos M., Christakis J. I., Bogdanos D., Tsimirika K., MacFarlane J., Goldberg Y. P., Sakellaropoulos N., Ganz T. and Nemeth E., Hepcidin in iron overload disorders. *Blood* 2005; 105 (10): 4103-5.

Park C. H., Valore E. V., Waring A. J. and Ganz T., Hepcidin, a urinary antimicrobial peptide synthesized in the liver. *J Biol Chem* 2001; 276 (11): 7806-10.

Peng J., Stanley A. J., Cairns D., Selby P. J. and Banks R. E., Using the protein chip interface with quadrupole time-of-flight mass spectrometry to directly identify peaks in SELDI profiles--initial evaluation using low molecular weight serum peaks. *Proteomics* 2009; 9 (2): 492-8.

Peters H. P., Laarakkers C. M., Swinkels D. W. and Wetzels J. F., Serum hepcidin-25 levels in patients with chronic kidney disease are independent of glomerular filtration rate. *Nephrol Dial Transplant* 2010; 25 (3): 848-53.

Petricoin E. F. and Liotta L. A., SELDI-TOF-based serum proteomic pattern diagnostics for early detection of cancer. *Curr Opin Biotechnol* 2004; 15 (1): 24-30.

Pietrangolo A., Dierssen U., Valli L., Garuti C., Rump A., Corradini E., Ernst M., Klein C. and Trautwein C., STAT3 is required for IL-6-gp130-dependent activation of hepcidin in vivo. *Gastroenterology* 2007; 132 (1): 294-300.

Pietrangolo A., Caleffi A. and Corradini E., Non-HFE hepatic iron overload. *Semin Liver Dis* 2011; 31 (3): 302-18.

Pineiro M., Alava M. A., Gonzalez-Ramon N., Osada J., Lasierra P., Larrad L., Pineiro A. and Lampreave F., ITIH4 serum concentration increases during acute-phase processes in human patients and is up-regulated by interleukin-6 in hepatocarcinoma HepG2 cells. *Biochem Biophys Res Commun* 1999; 263 (1): 224-9.

- Piperno A., Classification and diagnosis of iron overload. *Haematologica* 1998; 83 (5): 447-55.
- Piperno A., Girelli D., Nemeth E., Trombini P., Bozzini C., Poggiali E., Phung Y., Ganz T. and Camaschella C., Blunted hepcidin response to oral iron challenge in HFE-related hemochromatosis. *Blood* 2007; 110 (12): 4096-100.
- Piperno A., Galimberti S., Mariani R., Pelucchi S., Ravasi G., Lombardi C., Bilo G., Revera M., Giuliano A., Faini A., Mainini V., Westerman M., Ganz T., Valsecchi M. G., Mancina G. and Parati G., Modulation of hepcidin production during hypoxia-induced erythropoiesis in humans in vivo: data from the HIGHCARE project. *Blood* 2011; 117 (10): 2953-9.
- Pu X. P., Iwamoto A., Nishimura H. and Nagasawa S., Purification and characterization of a novel substrate for plasma kallikrein (PK-120) in human plasma. *Biochim Biophys Acta* 1994; 1208 (2): 338-43.
- Saguchi K., Tobe T., Hashimoto K., Sano Y., Nakano Y., Miura N. H. and Tomita M., Cloning and characterization of cDNA for inter-alpha-trypsin inhibitor family heavy chain-related protein (IHRP), a novel human plasma glycoprotein. *J Biochem* 1995; 117 (1): 14-8.
- Sala C., Ciullo M., Lanzara C., Natile T., Bione S., Massacane R., d'Adamo P., Gasparini P., Toniolo D. and Camaschella C., Variation of hemoglobin levels in normal Italian populations from genetic isolates. *Haematologica* 2008; 93 (9): 1372-5.
- Santini V., Girelli D., Sanna A., Martinelli N., Duca L., Campostrini N., Cortelezzi A., Corbella M., Bosi A., Reda G., Olivieri O. and Cappellini M. D., Hepcidin levels and their determinants in different types of myelodysplastic syndromes. *PLoS One* 2011; 6 (8): e23109.
- Siah C. W., Ombiga J., Adams L. A., Trinder D. and Olynyk J. K., Normal iron metabolism and the pathophysiology of iron overload disorders. *Clin Biochem Rev* 2006; 27 (1): 5-16.
- Silvestri L., Pagani A., Nai A., De Domenico I., Kaplan J. and Camaschella C., The serine protease matriptase-2 (TMPRSS6) inhibits hepcidin activation by cleaving membrane hemojuvelin. *Cell Metab* 2008; 8 (6): 502-11.
- Song J., Patel M., Rosenzweig C. N., Chan-Li Y., Sokoll L. J., Fung E. T., Choi-Miura N. H., Goggins M., Chan D. W. and Zhang Z., Quantification of fragments of human serum inter-alpha-trypsin inhibitor heavy chain 4 by a surface-enhanced laser desorption/ionization-based immunoassay. *Clin Chem* 2006; 52 (6): 1045-53.
- Suzuki H., Toba K., Kato K., Ozawa T., Tomosugi N., Higuchi M., Kusuyama T., Iso Y., Kobayashi N., Yokoyama S., Fukuda N., Saitoh H., Akazawa K. and Aizawa Y., Serum hepcidin-20 is elevated during the acute phase of myocardial infarction. *Tohoku J Exp Med* 2009; 218 (2): 93-8.
- Swinkels D. W., Girelli D., Laarakkers C., Kroot J., Campostrini N., Kemna E. H. and Tjalsma H., Advances in quantitative hepcidin measurements by time-of-flight mass spectrometry. *PLoS One* 2008; 3 (7): e2706.
- Tanno T., Bhanu N. V., Oneal P. A., Goh S. H., Staker P., Lee Y. T., Moroney J. W., Reed C. H., Luban N. L., Wang R. H., Eling T. E., Childs R., Ganz T., Leitman S. F., Fucharoen S. and Miller J. L., High levels of GDF15 in thalassemia suppress expression of the iron regulatory protein hepcidin. *Nat Med* 2007; 13 (9): 1096-101.
- Tanno T., Rabel A., Lee Y. T., Yau Y. Y., Leitman S. F. and Miller J. L., Expression of growth differentiation factor 15 is not elevated in individuals with iron deficiency secondary to volunteer blood donation. *Transfusion* 2010; 50 (7): 1532-5.
- Tavanti A., Maisetta G., Del Gaudio G., Petruzzelli R., Sanguinetti M., Batoni G. and Senesi S., Fungicidal activity of the human peptide hepcidin 20 alone or in combination with other antifungals against *Candida glabrata* isolates. *Peptides* 2011; 32 (12): 2484-7.

- Tessitore N., Girelli D., Campostrini N., Bedogna V., Pietro Solero G., Castagna A., Melilli E., Mantovani W., De Matteis G., Olivieri O., Poli A. and Lupo A., Heparin is not useful as a biomarker for iron needs in haemodialysis patients on maintenance erythropoiesis-stimulating agents. *Nephrol Dial Transplant* 2010; 25 (12): 3996-4002.
- Tomosugi N., Kawabata H., Wakatabe R., Higuchi M., Yamaya H., Umehara H. and Ishikawa I., Detection of serum hepcidin in renal failure and inflammation by using ProteinChip System. *Blood* 2006; 108 (4): 1381-7.
- Traglia M., Sala C., Masciullo C., Cverhova V., Lori F., Pistis G., Bione S., Gasparini P., Ulivi S., Ciullo M., Nutile T., Bosi E., Sirtori M., Mignogna G., Rubinacci A., Buetti I., Camaschella C., Petretto E. and Toniolo D., Heritability and demographic analyses in the large isolated population of Val Borbera suggest advantages in mapping complex traits genes. *PLoS One* 2009; 4 (10): e7554.
- Traglia M., Girelli D., Biino G., Campostrini N., Corbella M., Sala C., Masciullo C., Viganò F., Buetti I., Pistis G., Cocca M., Camaschella C., and Toniolo P., Association of HFE and TMPRSS6 genetic variants with iron and erythrocyte parameters is only in part dependent on serum hepcidin concentrations. *J Med Genet* 2011; 48 (9) :629-34.
- van Dijk B. A., Laarakkers C. M., Klaver S. M., Jacobs E. M., van Tits L. J., Janssen M. C. and Swinkels D. W., Serum hepcidin levels are innately low in HFE-related haemochromatosis but differ between C282Y-homozygotes with elevated and normal ferritin levels. *Br J Haematol* 2008; 142 (6): 979-85.
- van Winden A. W., Gast M. C., Beijnen J. H., Rutgers E. J., Grobbee D. E., Peeters P. H. and van Gils C. H., Validation of previously identified serum biomarkers for breast cancer with SELDI-TOF MS: a case control study. *BMC Med Genomics* 2009; 2 4.
- Verga Falzacappa M. V., Vujic Spasic M., Kessler R., Stolte J., Hentze M. W. and Muckenthaler M. U., STAT3 mediates hepatic hepcidin expression and its inflammatory stimulation. *Blood* 2007; 109 (1): 353-8.
- Villanueva J., Shaffer D. R., Philip J., Chaparro C. A., Erdjument-Bromage H., Olshen A. B., Fleisher M., Lilja H., Brogi E., Boyd J., Sanchez-Carbayo M., Holland E. C., Cordon-Cardo C., Scher H. I. and Tempst P., Differential exoprotease activities confer tumor-specific serum peptidome patterns. *J Clin Invest* 2006; 116 (1): 271-84.
- Walsh G. M., Rogalski J. C., Klockenbusch C. and Kast J., Mass spectrometry-based proteomics in biomedical research: emerging technologies and future strategies. *Expert Rev Mol Med* 2010; 12 e30.
- Wrighting D. M. and Andrews N. C., Interleukin-6 induces hepcidin expression through STAT3. *Blood* 2006; 108 (9): 3204-9.
- Xiao Z., Luke B. T., Izmirlan G., Umar A., Lynch P. M., Phillips R. K., Patterson S., Conrads T. P., Veenstra T. D., Greenwald P., Hawk E. T. and Ali I. U., Serum proteomic profiles suggest celecoxib-modulated targets and response predictors. *Cancer Res* 2004; 64 (8): 2904-9.
- Zhang Z., Bast R. C., Yu Y. H., Li J. N., Sokoll L. J., Rai A. J., Rosenzweig J. M., Cameron B., Wang Y. Y., Meng X. Y., Berchuck A., van Haaften-Day C., Hacker N. F., de Bruijn H. W. A., van der Zee A. G. J., Jacobs I. J., Fung E. T. and Chan D. W., Three biomarkers identified from serum proteomic analysis for the detection of early stage ovarian cancer. *Cancer Res* 2004; 64 (16): 5882-5890.
- Zhuo L., Hascall V. C. and Kimata K., Inter-alpha-trypsin inhibitor, a covalent protein-glycosaminoglycan-protein complex. *J Biol Chem* 2004; 279 (37): 38079-82.
- Zhuo L. and Kimata K., Structure and function of inter-alpha-trypsin inhibitor heavy chains. *Connect Tissue Res* 2008; 49 (5): 311-20.